Feasibility Study of 3D Printing of Concrete for Transportation Infrastructure

Final Report
September 2020

IOWA STATE UNIVERSITY
Institute for Transportation

Sponsored by
Iowa Highway Research Board
(IHRB Project TR-756)
Iowa Department of Transportation
(InTrans Project 18-674)

About the Institute for Transportation

The mission of the Institute for Transportation (InTrans) at Iowa State University is to develop and implement innovative methods, materials, and technologies for improving transportation efficiency, safety, reliability, and sustainability while improving the learning environment of students, faculty, and staff in transportation-related fields.

Iowa State University Nondiscrimination Statement

Iowa State University does not discriminate on the basis of race, color, age, ethnicity, religion, national origin, pregnancy, sexual orientation, gender identity, genetic information, sex, marital status, disability, or status as a US veteran. Inquiries regarding nondiscrimination policies may be directed to the Office of Equal Opportunity, 3410 Beardshear Hall, 515 Morrill Road, Ames, Iowa 50011, telephone: 515-294-7612, hotline: 515-294-1222, email: eooffice@iastate.edu.

Disclaimer Notice

The contents of this report reflect the views of the authors, who are responsible for the facts and the accuracy of the information presented herein. The opinions, findings and conclusions expressed in this publication are those of the authors and not necessarily those of the sponsors.

The sponsors assume no liability for the contents or use of the information contained in this document. This report does not constitute a standard, specification, or regulation.

The sponsors do not endorse products or manufacturers. Trademarks or manufacturers' names appear in this report only because they are considered essential to the objective of the document.

Iowa DOT Statements

Federal and state laws prohibit employment and/or public accommodation discrimination on the basis of age, color, creed, disability, gender identity, national origin, pregnancy, race, religion, sex, sexual orientation or veteran's status. If you believe you have been discriminated against, please contact the Iowa Civil Rights Commission at 800-457-4416 or the Iowa Department of Transportation affirmative action officer. If you need accommodations because of a disability to access the Iowa Department of Transportation's services, contact the agency's affirmative action officer at 800-262-0003.

The preparation of this report was financed in part through funds provided by the Iowa Department of Transportation through its "Second Revised Agreement for the Management of Research Conducted by Iowa State University for the Iowa Department of Transportation" and its amendments.

The opinions, findings, and conclusions expressed in this publication are those of the authors and not necessarily those of the Iowa Department of Transportation.

Technical Report Documentation Page

1. Report No.	2. Government Accession No.	3. Recipient's Catalog No.
IHRB Project TR-756		

4. Title and Subtitle	5. Report Date
Feasibility Study of 3D Printing of Concrete for Transportation Infrastructure	September 2020
	6. Performing Organization Code

7. Author(s)	8. Performing Organization Report No.
Kejin Wang (orcid.org/0000-0002-7466-3451), Kwangwoo Wi (orcid.org/0000-0001-9415-3187), Simon Laflamme (orcid.org/0000-0001-5666-3215), Sri Sritharan (orcid.org/0000-0001-9941-8156), Peter Taylor (orcid.org/0000-0002-4030-1727), and Hantang Qin (orcid.org/0000-0003-4180-7911)	InTrans Project 18-674

9. Performing Organization Name and Address	10. Work Unit No. (TRAIS)
Institute for Transportation Iowa State University 2711 South Loop Drive, Suite 4700 Ames, IA 50010-8664	11. Contract or Grant No.

12. Sponsoring Organization Name and Address	13. Type of Report and Period Covered
Iowa Highway Research Board Iowa Department of Transportation 800 Lincoln Way Ames, IA 50010	Final Report
	14. Sponsoring Agency Code IHRB Project TR-756

15. Supplementary Notes

Visit https://intrans.iastate.edu/ for color pdfs of this and other research reports.

16. Abstract

Three-dimensional (3D) printing concrete technology has already been adopted for structural applications. Many houses and pedestrian bridges have been 3D printed in the US and other countries. In spite of exploratory applications, 3D concrete printing technology remains fragmentary, and its full-scale uses in transportation infrastructure are still rarely seen. In order to bring the full benefits of this technology to the construction industry, it still requires a much better understanding of the relationships among digital design, operation/processing, mechanisms of building materials, formulation of printing materials, and performance of printed products. The present study aimed at exploring the feasibility of developing 3D printable concrete mixtures and evaluating their potential uses for transportation infrastructure.

In this project, a commercial 3D clay printer was used to print small-scale clay, paste, and mortar objects. The effects of printing parameters and procedures, printable materials, and mix proportions on printing properties, such as flowability, extrudability, printability, buildability as well as on mechanical properties (compressive and tensile strength) of printed objects, were investigated. The methods for characterizing the quality of 3D printed objects were examined.

The results indicate that paste and mortar mixtures made with cement, silica fume, a rapid-set grout powder, viscosity modifying agents (VMAs), and superplasticizer can be engineered to have desirable flowability, extrudability, printability, and buildability for 3D printing. Samples that were 3D printed with different printing paths and tested under different loading direction showed clear anisotropic behavior in their mechanical properties. Printing qualities, such as geometric accuracy, distortion, surface roughness, etc., of printed objects can be well evaluated using image analysis. In addition, a qualitative ranking system was also developed for evaluation of the printing qualities of 3D concrete printing.

17. Key Words	18. Distribution Statement
3D concrete printing technology—3D printing—additive manufacturing—concrete manufacturing—concrete mixtures—printing qualities	No restrictions.

19. Security Classification (of this report)	20. Security Classification (of this page)	21. No. of Pages	22. Price
Unclassified.	Unclassified.	67	NA

Form DOT F 1700.7 (8-72) **Reproduction of completed page authorized**

FEASIBILITY STUDY OF 3D PRINTING OF CONCRETE FOR TRANSPORTATION INFRASTRUCTURE

Final Report
September 2020

Principal Investigator
Kejin Wang, Professor
Civil, Construction, and Environmental Engineering, Iowa State University

Co-Principal Investigators
Simon Laflamme, Associate Professor
and Sri Sritharan, Professor
Civil, Construction, and Environmental Engineering, Iowa State University
Peter Taylor, Director
National Concrete Pavement Technology Center, Iowa State University
Hantang Qin, Assistant Professor
Industrial and Manufacturing Systems Engineering, Iowa State University

Research Assistants
Kwangwoo Wi and Karthick Manikandan

Authors
Kejin Wang, Kwangwoo Wi, Simon Laflamme, Sri Sritharan, Peter Taylor, and Hantang Qin

Sponsored by
Iowa Highway Research Board and
Iowa Department of Transportation
(IHRB Project TR-756)

Preparation of this report was financed in part
through funds provided by the Iowa Department of Transportation
through its Research Management Agreement with the
Institute for Transportation
(InTrans Project 18-676)

A report from
Institute for Transportation
Iowa State University
2711 South Loop Drive, Suite 4700
Ames, IA 50010-8664
Phone: 515-294-8103 / Fax: 515-294-0467
https://intrans.iastate.edu/

TABLE OF CONTENTS

ACKNOWLEDGMENTS ix

EXEUTIVE SUMMARY xi

1. INTRODUCTION 1

1.1 Research Background 1
1.2 Objectives 2
1.3 Scope and Tasks 2

2. LITERATURE REVIEW 4

2.1 General Information on 3D Concrete Printing 4
2.2 Key Properties of 3D Printing Concrete 4
2.3 Materials and Mix Proportions of 3D Printing Concrete 5
2.4 Effects of Other Cementitious Materials and Additives 6
2.5 Effects of Admixtures 7

3. INITIAL TRIAL OF 3D PRINTING 10

3.1 Materials 10
3.2 Mix Design and Procedure 11
3.3 Printing Procedure and Test Methods 11
3.4 Test Results 12
3.5 Summary 14

4. PRINTER SELECTION AND PRINTING PARAMETER STUDY 15

4.1 Introduction of 3D Printer 15
4.2 Printing Parameter Study 16
4.3 Summary 21

5. 3D PRINTING CONCRETE MIX DESIGN AND OPTIMIZATION 22

5.1 Materials 22
5.2 Mix Proportions and Mixing Procedure 23
5.3 Printing Parameters and Procedure 24
5.4 Evaluation Methods 25
5.5 Test Results 26

6. MIXTURE CHARACTERIZATION AND PROPERTIES OF 3D PRINTED PRODUCTS 30

6.1 Overview 30
6.2 Materials, Mix Proportions, and Procedure 30
6.3 Printing Parameters and Procedure 30
6.4 Test Methods 31
6.5 Test Results 33

7. OBJECT DESIGN AND QUALITY EVALUATION 39

7.1 Object Design 39
7.2 Printing Quality Evaluation 40

8. SUMMARY, CONCLUSION, AND FUTURE STUDY....46
8.1 Summary....46
8.2 Conclusions....47
8.3 Further Study....49
REFERENCES....51

LIST OF FIGURES

Figure 3.1. Syringe and printing path 12
Figure 3.2. Effects of VMA on the 3D printing by syringe 12
Figure 3.3. Effects of superplasticizer on the 3D printing by syringe 13
Figure 3.4. Effects of chemical admixtures on the printing qualities of mixtures with silica fume 13
Figure 3.5. Pop outs by air bubbles in the syringe 14
Figure 4.1. 3D printer used in this study 15
Figure 4.2. 3D modeling images 17
Figure 4.3. Effects of different printing speeds on the printing qualities 18
Figure 4.4. Effects of different extrusion speeds on the printing qualities 19
Figure 4.5. Effects of printing speed and extrusion speed on the layer width 19
Figure 4.6. Effects of infill rates on the printing qualities 20
Figure 4.7. Problems during clay printing process 21
Figure 5.1. Strength development of grout used 23
Figure 5.2. 3D modeling image 24
Figure 5.3. Curing method 25
Figure 5.4. Effects of VMA and superplasticizer on concrete printing 26
Figure 5.5. Effects of the grout and superplasticizer on the concrete printing 27
Figure 5.6. Effects of w/b on the concrete printing 27
Figure 5.7. Effects of printing speed on the printing qualities 28
Figure 5.8. Problems during concrete printing process 29
Figure 6.1. Sample preparation for mechanical properties 32
Figure 6.2. Cut samples for mechanical properties 32
Figure 6.3. Buildability of printable mortars illustrated by the shape of printed objects 34
Figure 6.4. Failures during direct tension tests 35
Figure 6.5. Compressive strength at 7 and 28 days 35
Figure 6.6. Failure modes of samples under compression tested at 28 days 36
Figure 6.7. Flexural strength at 7 and 28 days 37
Figure 6.8. Failure modes of samples under flexural load tested at 28 days 38
Figure 7.1. Different objects printed with clay and concrete 39
Figure 7.2. Printing quality evaluation and comparison 41
Figure 7.3. Photos and 3D-SLSS images of 3D printed clay samples 42
Figure 7.4. Illustration of 2D plot development from 3D-SLSS images of a 3D printed sample 43
Figure 7.5. 3D-SLSS measurements of geometric parameters of 3D printed samples 44

LIST OF TABLES

Table 2.1. Definition of key properties in 3D printing concrete 5
Table 2.2. Frequency of w/b ratios used in studies on 3D printing concrete 5
Table 2.3. Frequency of s/b ratios used in studies on 3D printing concrete 6
Table 2.4. Effects of SCMs on the properties of 3D printing concrete 7
Table 2.5. Effects of admixtures on the properties of 3D printing concrete 8
Table 3.1. Materials and their sources 10
Table 3.2. Chemical composition of cementitious materials 10
Table 3.3. Mix proportion for initial trial 11
Table 4.1. Physical and chemical properties of clay 16
Table 4.2. Printing parameters for clay printing 16
Table 4.3. Printing parameters for clay printing 17
Table 5.1. Fluidity and setting time of grout 22
Table 5.2. Mix proportion for 3D printable concrete 23
Table 5.3. Printing parameters for concrete printing 24
Table 6.1. Mix proportion with different replacement ratio of grout 30
Table 6.2. Results from flow table test 33

ACKNOWLEDGMENTS

The authors would like to acknowledge the Iowa Department Transportation (DOT) and Iowa Highway Research Board (IHRB) for their sponsorship for this study. Valuable input on the project activities and comments on this report from the technical advisory committee (TAC) members, Ahmad Abu-Hawash, Michael Nop, and Kimball Olson, are also greatly appreciated. Special thanks to Ted Huisman with the Iowa State University Department of Civil, Construction, and Environmental Engineering for his help on three-dimensional (3D) printer setup, Joseph Schaefer with the Department of Aerospace Engineering (strength test) for their help on mechanical tests, and Bowen Li and Vignesh Suresh with the Department of Mechanical Engineering for their help on image analysis in quantifying the quality of printed objects.

EXEUTIVE SUMMARY

Recently, there has been a growing interest in the use of three-dimensional (3D) printing technology in concrete manufacturing. Instead of placing, leveling, consolidating, and finishing concrete, 3D concrete printing technology brings all the traditional manufacturing steps into one process by adding a building material to itself with automation and digitalization. 3D printing technology also permits the creation of concrete structures having complex geometry (e.g., various shapes and cross sections) with high precision. It enables concrete construction under extreme conditions that are difficult and/or very costly for conventional concrete construction to have traditional formwork setup, placing, and/or consolidation. Using such an innovative technology can significantly alter the way society constructs today, facilitating immense time and cost savings in construction and opening a new door for innovation in structural concrete design and construction.

However, in spite of exploratory applications, 3D concrete printing technology remains fragmentary, and its full-scale uses in transportation infrastructure are still rarely seen. In order to bring the full benefits of this technology to the construction industry, it still requires a much better understanding of the relationships among digital design, operation/processing, mechanisms of building materials, formulation of printing materials, and performance of printed products. The present study aimed at exploring the feasibility of developing 3D printable concrete mixtures and evaluating their potential uses for transportation infrastructure.

The specific objectives of this project included the following:

1. Develop a printable and functional 3D printing concrete mixture
2. Characterize the 3D printed concrete properties and have a better understanding of the concrete behavior
3. Explore the potential applications of 3D printed concrete in the field of transportation engineering, realize the challenges and future perspectives, and lay a foundation for extended studies and applications of 3D printed concrete in Iowa

The following activities were performed in this project:

1. *Literature review* – Based on the information collected from existing publications, key properties of fresh 3D printing concrete, such as flowability, extrudability, printability, buildability, and open time, were defined, and their testing methods were defined. Materials and proportions of typical 3D printing concrete mixes were reviewed, and the effects of different types of materials on the required properties for 3D printing concrete were comprehended, and related information was adopted in the mix design and evaluation of the present study.

2. *Printing procedure and parameter study* – A commercial 3D clay printer (3D potter bot) was selected and used to print small-scale clay and concrete objects in this study. Due to its small size, only paste and mortar were printed in the present study. Printer setup (selections of nozzle size and shape, stand-off distance, etc.), different printing parameters (printing and extrusion speed), and printing procedures (material preparation, loading time, and printing time) were also investigated.

3. *Design of 3D printable mortar mixtures* – Based on the information collected from the literature review, different types of materials, including cement, silica fume, viscosity modifying agents (VMAs), and superplasticizer, and different water-to-binder (w/b) ratios were selected for design of 3D printing mixtures. Trial and error tests were conducted to identify paste and mortar mixtures with proper flowability that are suitable for being placed in the printer, extruded out, and printing well-shaped filaments layer-by-layer easily and mixtures with proper thixotropic behavior for holding the shape of printed objects. A commercially available highly flowable, rapid-set grout was used to facilitate the mixtures to reach the desired 3D printing properties.

4. *3D printable mix optimization* – The effects of materials, mix proportions, and printing parameters on fresh printable concrete properties, such as flowability, extrudability, printability, and open time, were investigated. Based on the easiness of the printing processes and the quality of the printed objects, the optimal mortar mix was identified.

5. *Design of 3D printing objects* – Small-scale samples with simple geometries, such as circular columns, cubes, and prisms, with different infill rates (0%, 60%, and 80%), were printed with clay, pastes, and mortar in the present study.

6. *3D printed concrete performance* evaluation – Mechanical properties (compressive and flexural strength) of printed objects made with various mortar mixtures were measured. Samples were 3D printed with different printing paths and tested under different loading directions to understand the anisotropic behavior of the printed objects. Printing qualities of the printed objects were evaluated using image analysis.

The following are the major finding obtained from the present project:

1. Materials had significant effects on key printing properties, including flowability, extrudability, buildability, and open time, of the 3D printing mortar. Use of silica fume and VMAs decreased flowability and extrudability but increased buildability and shape-holding ability. Increase in the dosage of superplasticizer enhanced flowability and extrudability, but it decreased buildability. Use of a highly flowable, rapid-set grout significantly accelerated the setting behavior of the mortar mixtures, leading to enhanced buildability.

2. Mix proportions also significantly influenced printing properties. Mixtures with a very low w/b ratios showed unacceptable flowability and extrudability, causing difficulty in feeding mortars into the extruder or blockage at the nozzle tip. Increase in the w/b ratio generally led to increased flowability and extrudability of 3D printing mortar mixtures. However, excessive flowability could result in structural deformation, such as slump, of the printed objects, thus reducing buildability. Based on the test results, Mix 0.32-G20, made with a binder containing portland cement, silica fume (2.5% by weight of binder), and 20% grout, and a w/b ratio of 0.32, was the best mortar mixture among all mixtures studied. This mixture was easily placed into the printer, extruded out smoothly and consistently, and able to hold the shape of the designed objects during and after printing.

3. Several defects were identified during the 3D concrete printing, and they were (a) air bubble pop outs, (b) discontinuity, (c) slumping, and (d) cracking. The first three were largely related to the flow behavior of the 3D printing concrete mixtures, while the last one was mainly due to plastic shrinkage. Prompt and proper curing is essential for 3D printing concrete in order to reduce slump and plastic shrinkage cracking.

4. The compressive and flexural strength of the 3D printing mortar samples printed with different printing paths were measured under different loading directions, and the results were compared with those of mold-cast samples made with the same mortar mixture. It was found that the mold-cast samples had a higher compressive strength than the printed samples regardless of loading directions. This might be attributed to the existence of weak interlayers between printed filaments. However, under flexural loading, the printed samples had a higher flexural strength than the mold-cast sample regardless of loading directions. This might be because the mixtures were densified during the 3D printing/extrusion process, leading to higher flexural strength when the 3D printed samples were loaded in the direction perpendicular to the filaments. However, little explanation could be made on why the 3D printed samples had higher flexural strength than the cast samples when they were loaded parallel to the filaments.

5. The 3D printed samples displayed different compressive and flexural strength values when loaded in different directions, which clearly evidenced anisotropic behavior of the bulk material. The compressive strength of the 3D printed samples loaded in the direction parallel to the filaments was much lower than that of the corresponding samples loaded in the direction perpendicular to the filaments, which was probably due to potential buckling of the filaments under compression. However, the difference in flexural strength of the 3D printed samples loaded in the two different directions was much smaller.

6. In order to evaluate the quality of the 3D printed concrete objects, a qualitative ranking system based on visual inspection was developed in the present study. Based on this ranking system, the samples printed with the best mortar mixtures used in the present study could be ranked as 2 (the second to the best) out of 5, since they showed uniform layers and a bit of a rough surface. Quantitative evaluation for the printing qualities was also conducted with a 3D structured light scanning system (3D-SLSS). The results showed that all the printed samples exhibited certain differences between their measured and designed values, even for those that appeared well-printed. Compared with the designed object, the printed samples generally had reduced total height, diameter, and layer thickness but increased layer width, mainly due to slump. In addition to printing materials (concrete mixtures), various printing parameters, including printing speed, extrusion speed, nozzle size and shape, stand-off distance, etc., could affect printing qualities of 3D printed objects. These affecting parameters should be further studied to improve 3D printing quality.

1. INTRODUCTION

1.1 Research Background

Recently, there has been a growing interest in the use of three-dimensional (3D) printing technology in concrete manufacturing. Instead of placing, leveling, consolidating, and finishing concrete, 3D concrete printing technology brings all the traditional manufacturing steps into one process by designing and building full-scale concrete objects in the laboratory with automation and digitalization. 3D printing technology also permits the creation of concrete structures having complex geometry (e.g., various shapes and cross sections) with high precision. It enables concrete construction under extreme conditions that are difficult and/or very costly for conventional concrete construction to have traditional formwork setup, placing, and/or consolidation. Using such an innovative technology can significantly alter the way society constructs today, facilitating immense time and cost savings in construction and opening a new door for innovation in structural concrete design and construction.

The 3D printing process employs an additive manufacturing (AM) process whereby products are built from a digital model on a layer-by-layer basis. The first application of 3D printing technology for concrete construction can be dated to 1998 when Khoshnevis introduced a technique termed contour crafting to build a structural component layer-by-layer using a crane and a robotic arm (Khoshnevis and Dutton 1998, Khoshnevis 2004). Since then, various types of houses, bridges, and architectural elements have been built using layer-by-layer 3D printing methods, also called additive manufacturing (Sevenson 2015, Malaeb et al. 2015, ArchDaily 2017, Massachusetts Institute of Technology 2017).

Recently, applications of 3D concrete printing technology have been extended to transportation infrastructure. In 2017, the world's first 3D printed pedestrian bridge (12 m long by 1.75 m wide) was constructed using microfiber-reinforced concrete in the urban park of Castilla-La Mancha, Madrid, Spain (Institute for Advanced Architecture of Catalonia 2017). In 2018, two robots completed a 3D printed steel bridge with a span for the Amsterdam Canal (Block 2018). In the US, the U.S. Marine Corps 3D printed a 500 ft^2 concrete barrack room at the U.S. Army Engineer Research and Development Center in Champaign, Illinois, in only 40 hours (Rogers 2018). Later, the U.S. Marines successfully 3D printed the first reinforced concrete bridge in the US at Camp Pendleton, California, within only 14 hours (Harkins 2019). In 2019, the world's largest 3D printed concrete bridge (26.3 m long by 3.6 m wide) was completed in Shanghai, China, which was built within 420 hours (Ravenscroft 2019).

In spite of exploratory applications, 3D concrete printing technology remains fragmentary, and its full-scale uses in transportation infrastructure are still rarely seen. In order to bring the full benefits of this technology to the construction industry, it still requires a much better understanding of the relationships among digital design (e.g., automation for complicated structures), operation/processing (e.g., optimization of printer setup and printing procedure), mechanisms of build (e.g., requirements for extrudability and shape stability), formulation of printing materials (e.g., mixture proportioning for adequate workability and solidification behavior), and performance of printed products (e.g., strength and durability). The present study

aimed at exploring the feasibility of developing 3D printable concrete mixtures and evaluating their potential uses for transportation infrastructure.

1.2 Objectives

The goal of the present study was to apply 3D concrete printing technology to transportation-related infrastructure. The specific objectives of this projects were as follows:

- Develop a printable 3D concrete printing mixture using materials commonly available in Iowa
- Better understand the requirements of 3D printing technology for concrete mixture behavior
- Characterize the 3D printed concrete properties and evaluate the potential of 3D printed concrete for the field of transportation engineering

1.3 Scope and Tasks

To accomplish the above-mentioned goal and objectives, the main scope of this project was set to develop and evaluate printable concrete mixtures using available concrete materials and a commercial 3D printer. The following major tasks were performed:

Task 1: Literature review – A literature review was conducted covering 3D printing methods, equipment, materials, processes, and characterizations of printed products.

Task 2: 3D printer selection – Based on the literature review results, a laboratory-scale concrete printer was selected, purchased, and used in the project.

Task 3: Design of 3D concrete printing mixtures – Based on the literature review results, several sets of paste and mortar mixes were designed with various materials, water-to-binder (w/b) ratio, and additives/admixtures. These mixes were evaluated according to Task 5.

Task 4: Design of 3D printing objects – Commonly used computer software was employed to automate simple 3D objects, like cylinders and prisms, which were then cut to form cubes and beams for mechanical property and microstructure evaluations.

Task 5: Characterization and performance evaluation of 3D printed concrete – The characterizations and evaluations were focused on fresh concrete mixtures, which included flowability, printability, and buildability or shape stability). The key engineering properties (e.g., compressive sand flexural strength and anisotropic behavior) of the printed samples were also evaluated in comparison with the mold-cast samples.

Task 6: Data analysis – In addition to compiling all testing data, the effects of key mix design parameters, e.g., w/b ratio and additive/admixture content, on properties of printed concrete were identified. The criteria for accepting the 3D concrete printing mixes and the feasibility of using 3D concrete printing for structural components were considered.

Task 7: Final project report – This final project report includes a summary of the literature

review, details on concrete mix proportions, test methods, and performance properties of printed concrete. It also includes the conclusions from the data analysis as well as recommendations for extended studies and potential transportation applications of 3D concrete printing technology in the field of transportation engineering.

2. LITERATURE REVIEW

2.1 General Information on 3D Concrete Printing

As mentioned previously, 3D concrete printing technology was first reported in 1998, when Dr. Khoshnevis at the University of Southern California (USC) printed a concrete wall component using an AM process with a contour crafting system (Khoshnevis and Dutton 1998). Since then, many applications of 3D concrete printing technology have been reported. Although still in its infancy stage, studies of 3D concrete printing have been rapidly extended to the printing of reinforced concrete, fiber-reinforced concrete, high-performance concrete, and prestressed concrete over the past couple of years (Ogura et al. 2018).

In principle, a 3D concrete printing process uses 3D modeling software that slides and represents the object to be printed as a series of two-dimensional (2D) layers and exports the data to a printing machine, which prints the object layer-by-layer directly onto targeted areas. There are several approaches to conduct a 3D printing process. One is a contour crafting process, where nozzles are used to extrude concrete materials for printing, and trowels are used to shape the printed layers, thus creating smooth and accurate planar and free-form surfaces. Another is a modern 3D printing process, where only a print head is used for concrete deposition/extrusion (Zhang et al. 2019). The modern 3D printer is simple and easy to operate, and it is commonly used and can provide more opportunities for concrete mix design studies.

2.2 Key Properties of 3D Printing Concrete

Research has indicated that in addition to the proper printing equipment and automation design tools, a core requirement for a successful 3D printed concrete project is a desirable and robust "ink," i.e., an engineered concrete mixture. Presently, most 3D concrete mixtures are designed by trial and error, and the performance of the mixtures depends largely upon the equipment used (nozzle size and applied pressure) as well as the configurations and dimensions of the objects to be printed. Optimization of the concrete mixtures is now mainly based on early age concrete properties, such as flowability, extrudability, printability, buildability, and open time. Table 2.1 shows the key properties of 3D printable concrete defined in several studies.

Table 2.1. Definition of key properties in 3D printing concrete

Properties	Definition	Ref.
Flowability	The level of ease of moving a printing material from a mixer (via a storage tank) to the nozzle of a printer	Malaeb et al. 2015
Extrudability	The ability for material to be extruded out of the nozzle of a printer smoothly and consistently	Wu et al. 2016
Printability	The ease, consistency, and reliability of deposition of a printing material through a deposition device	Lim et al. 2012
Buildability	The ability of a printed filament to maintain its shape under the weight of subsequently printed layers during and after the printing process	Soltan and Li 2018
Open time	The period of time in which the workability is consistent within certain tolerances acceptable for 3D printing	Lim et al. 2012

It should be noted that the requirements for flowability, printability, extrudability, buildability, and open time of 3D printable concrete mixtures vary with the features of the printer used and the objects to be printed, and they also differ with printing parameters (deposition distance, extrusion speed, and printing speed) and printing procedure (loading of printing material and design of printing paths) used. Therefore, 3D printing concrete mixtures should be designed and adjusted to fit these features, parameters, and procedures. Among the properties listed in Table 2.1, extrudability and buildability are the most important, but they are inherently in conflict. Good extrudability requires certain flowability, while good buildability demands a high resistance to flow or deformation. However, for successful 3D concrete printing, both properties must be achieved at the same time.

2.3 Materials and Mix Proportions of 3D Printing Concrete

In order to develop a mix design for 3D printable concrete, a wide variety of mix proportions has been reported, and Tables 2.2 and 2.3 show the frequency of w/b and sand-to-binder (s/b) ratios used in different mix designs used in studies.

Table 2.2. Frequency of w/b ratios used in studies on 3D printing concrete

w/b	Frequency (%)
w/b <0.2	0.3
0.2 < w/b < 0.3	23.3
0.3 < w/b < 0.4	37.5
0.4 < w/b < 0.5	17.7
0.5< w/b	11.2

Table 2.3. Frequency of s/b ratios used in studies on 3D printing concrete

s/b	Frequency (%)
s/b <0.5	4.3
0.5 < s/b < 1.0	10.8
1.0 < s/b < 1.5	41.5
1.5 < s/b < 2.0	19.8
2.0 < s/b < 2.5	21.2
2.5 < s/b	2.4

The most frequently used w/b ratio was 0.30–0.40, and 0.20–0.30 was the second most frequently used in mix proportions for 3D printable concrete, as shown in Table 2.2. This could be due to the fact that a low w/b ratio could accelerate the cement hydration and reduce empty spaces in a cementitious matrix after water evaporates. These low w/b ratios inevitably require the usage of a superplasticizer that attaches on the surface of particles and leads to well-dispersed cementitious materials. This is because 3D printable concrete should have high flowability to be transported through the delivery system and smoothly extruded.

It has been reported that the s/b ratio affects the rheological and mechanical properties of 3D printable concrete; the frequency of s/b used in studies on the 3D printing concrete was presented previously in Table 2.3. The most frequently used s/b ratio was 1.0–1.5, and s/b ratios of 1.5–2.0 and 2.0–2.5 were also frequently used in mix designs of 3D printable concrete. The mixture with a high s/b generally has high yield stress or low flowability due to high interparticle friction (Ogura et al. 2018, Zhang et al. 2019).

2.4 Effects of Other Cementitious Materials and Additives

In order to achieve fast stiffness and strength development for buildability, geopolymers and different types of cement, such as rapid-setting cement, calcium aluminate cement (CAC), and calcium sulfoaluminate cement (CSA), have been used (Soltan and Li 2018, Khalil et al. 2017, Ma et al. 2018).

Supplementary cementitious materials (SCMs), such as fly ash and silica fume, have been widely employed in 3D printing concrete, as they significantly affect the properties of 3D printable concrete.

Additives, like limestone powder and gypsum, have been used to enhance the performance of 3D printing concrete The effects of some SCMs and additives on the key properties are presented in Table 2.4.

Table 2.4. Effects of SCMs on the properties of 3D printing concrete

Materials	Effects	Ref.
Fly ash	To enhance flowability and maintain consistent viscosity with increased time	Lee et al. 2018, Ahmaruzzaman 2010
Silica fume	To accelerate cement hydration and increase yield stress and viscosity	Ma et al. 2017, Benaicha et al. 2015
Limestone powder	To densify the microstructure and control the hydration of cementitious paste	Bentz et al. 2019, Oey et al. 2013
Gypsum	To accelerate the setting behavior	Vaitkevičius et al. 2018, Kovler 1998

The spherical shape of fly ash can enhance the flowability of 3D printable concrete by the ball bearing effect, and this leads to decreased water requirements for a given slump. According to Lee et al. (2018), mixtures with 30% of fly ash led to only a 2% reduction in viscosity; whereas, ordinary portland cement (OPC) showed a 32% reduction in viscosity. This result indicates that the open time for 3D printable concrete can be extended by using fly ash in the mix design.

Silica fume has been widely used in different types of concrete, since it can increase the segregation resistivity and early strength. Due to its very fine particle size and large surface area, it accelerates the cement hydration and fills fine gaps in a cementitious matrix (Mehdipour and Khayat 2017). In addition, the large surface area of silica fume leads to high water absorption and the formation of flocculation structures in the cement matrix; thus, it increases the yield stress and viscosity (Benaicha et al. 2015, Mehdipour and Khayat 2017).

Limestone powder is widely used in concrete, and especially in self-consolidating concrete. It has been reported that limestone powder can influence concrete performance through filler, nucleation, and chemical effects (Berodier and Scrivener 2014). The filler effect leads to a densified microstructure. The nucleation effect accelerates cement hydration (with the chemical effort, forming hemi- or mono-carboaluminates by reacting with aluminates in cement, stabilizing ettringite, and further reducing porosity of cement matrix) (Wang et al. 2018).

Gypsum is normally added into cement during the clinker grinding process to control the setting behavior of cement. According to Vaitkevičius et al. (2018), the final set time was decreased from 20 to 16 min when the gypsum-to-cement ratio increased from 20% to 60%. Caution should be taken when gypsum is used to control setting. Dosage is very dependent on cement chemistry, and negative side effects such as flash/false set and even later expansions can be significant.

2.5 Effects of Admixtures

Various admixtures have been explored to enhance the rheological properties of 3D printable concrete, and it is crucial to balance the two conflicting rheological properties: high flowability and high thixotropy. As a result, most 3D printable concrete contains both superplasticizer and

viscosity modifying agents (VMAs). In addition, accelerator and retarder have been used, and the detailed effects of these materials are presented in Table 2.5.

Table 2.5. Effects of admixtures on the properties of 3D printing concrete

Materials	Effects	Ref.
VMAs	To improve dimension stability and segregation resistance	Kazemian et al. 2017
Superplasticizer	To enhance flowability	Mardani-Aghabaglou et al. 2013, Chandra and Björnström 2002
Accelerator	To accelerate setting behavior and enhance buildability	Malaeb et al. 2015, Le et al. 2012a
Retarder	To delay setting behavior and extend open time	Malaeb et al. 2015, Zhang et al. 2018

VMAs have been increasingly used in self-consolidating concrete (SCC) due to their unique properties, such as enhancements in segregation resistance. and water retention. VMAs can be divided in to two groups: inorganic and organic. Nanoclay and nanosilica are the most representative materials in inorganic VMAs. Natural or synthetic polymers are included in organic VMAs. One of the organic VMAs, hydroxypropyl methylcellulose (HPMC), has been reported in several studies (Zhi et al. 2018).

As mentioned previously, a low w/b ratio has been preferred by most 3D concrete printing studies. In addition to an increase in concrete strength, a low w/b concrete also provides a high yield stress for the concrete to hold its shape after being extruded. However, before being extruded out, concrete mixtures must be sufficiently flowable to be placed into a printer and extruded out easily. Therefore, the use of a superplasticizer is often necessary in a 3D printable concrete mixture. It should be noted that extensive usage of a superplasticizer can also lead to the retardation of cement hydration, since the polymers in a superplasticizer attach onto the surface of cement particles and prevent them from reacting with water (Leemann and Winnefeld 2007).

An accelerator speeds up cement hydration and results in early setting and early strength development of concrete. Accelerators have been widely used in concrete repair, which requires the fast evolution of mechanical properties. In 3D printing concrete use of an accelerator helps freshly extruded concrete to hold its shape, thus, increasing buildability. There is a concern that use of an accelerator may decrease the extrudability due to the fast cement hydration . To overcome this shortage, Maleab et al. (2015) added an accelerator right before extrusion and found its effect on the flowability was minor, although the cement hydration was enhanced.

It has been reported that the usage of a retarder significantly affected both flowability and buildability depending on the dosage. According to Zhang et al. (2018), the mixture with retarder showed the lowest loss of flowability among samples, and it led to extended open time. The effects of retarder on the mechanical properties of 3D printable concrete were found in the study by Le et al. (2012b), and it indicated that use of more than 1% (by weight of binder) of retarder

decreased the early compressive strength; however, its effect on later mechanical properties was minimal.

3. INITIAL TRIAL OF 3D PRINTING

The initial trial tests were performed while the research team was waiting for the delivery of a commercial 3D concrete printer. Therefore, instead of a 3D printer, a plastic syringe was used to print objects manually and to simulate a 3D printing process. The objective of the initial trial for 3D printing was to get familiar with the behavior of pastes made with different materials and mix proportions and to select mix candidates for the commercial 3D concrete printer.

3.1 Materials

Materials for 3D printing concrete used in this study included cementitious materials and chemical admixtures. The types and source of these materials are listed in Table 3.1.

Table 3.1. Materials and their sources

Materials	Type	Source
Cementitious materials		
Portland cement	Type I/II	Ash grove
Silica fume	Eucon MSA	Euclid
Chemical admixtures		
VMA	Vmar-3	GCP Applied Technologies
Superplasticizer (SP)	Eucon 1037	Euclid

3.1.1 Cementitious Materials

Cementitious materials used in this study include Type I/II portland cement and silica fume. Their chemical compositions are presented in Table 3.2.

Table 3.2. Chemical composition of cementitious materials

	Raw materials	
Oxides (%)	**Portland cement**	**Silica fume**
SiO_2	20.1	97.10
Al_2O_3	4.4	0.20
Fe_2O_3	3.1	-
SO_3	2.8	0.25
CaO	64	0.81
MgO	2.22	0.13
Na_2O	0.14	0.17
K_2O	0.58	0.80

3.1.2 Chemical Admixtures

Two different admixtures, a VMA and superplasticizer, were used to prepare a 3D printable paste for the initial trial.

3.2 Mix Design and Procedure

Table 3.3 shows the mix proportions of the initial trial tests for 3D printing concrete using a plastic syringe.

Table 3.3. Mix proportion for initial trial

Mix ID	w/b	Cement	Silica fume	VMA (binder %)	Superplasticizer (binder %)
C100-V0.5-SP0.5	0.30	100	-	0.5	0.5
C100-V1.0-SP0.5	0.30	100	-	1.0	0.5
C100-V1.5-SP0.5	0.30	100	-	1.5	0.5
C100-V1.0-SP0.75	0.30	100	-	1	0.75
C100-V1.0-SP1.0	0.30	100	-	1	1
C100-V1.0-SP1.25	0.30	100	-	1	1.25
C97.5-SF2.5-V0.5-SP1.0	0.30	97.5	2.5	0.5	1
C97.5-SF2.5-V1.0-SP1.0	0.30	97.5	2.5	1	1
C97.5-SF2.5-V1.0-SP1.25	0.30	97.5	2.5	1	1.25

The sum of binder (cement+silica fume) is 100. The Mix IDs describe the proportion of cement (C), silica fume (SF), VMA (V), and superplasticizer (SP) for each test.

All the dry powder (cement and silica fume) was mixed for 3 min to prevent the agglomeration of particles, and then half the water and all the superplasticizer were added and mixed for 1 min. Then, the rest of water and VMA were added and mixed for 1 min. Finally, the complete mixtures were mixed for 3 min. The total mixing time was 8 min including the dry mix.

3.3 Printing Procedure and Test Methods

A plastic syringe was used to print the 3D printable paste to simulate the real 3D printing process. The pastes were poured into the syringe, and hand-tamping was conducted to eliminate air bubbles in the syringe. Then, based on the printing path shown in Figure 3.1b, the mixtures were printed with a constant speed.

(a) Plastic syringe (100 ml)

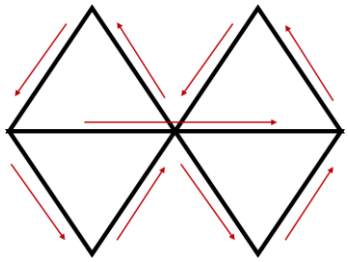

(b) Printing path

Figure 3.1. Syringe and printing path

When the mixtures could not be extruded or the printed layers started to be deformed, the printing process was stopped. Then, a visual inspection was conducted to check the printing qualities of the printed samples.

3.4 Test Results

Figure 3.2 shows the effects of the VMA dosage has on the printing qualities.

(a) C100-V0.5-SP0.5

(b) C100-V1.0-SP0.5

(c) C100-V1.5-SP0.5

The Mix IDs describe the proportion of cement (C), VMA (V), and superplasticizer (SP) for each test.

Figure 3.2. Effects of VMA on the 3D printing by syringe

As the dosage of VMA increased, the mixture became more difficult to be extruded from the syringe because the flowability of the mixture decreased with the increased viscosity as the VMA dosage increased. Therefore, extrudability decreased, and the total number of deposited layers eventually decreased.

Figure 3.3 illustrates the effects of superplasticizer on the printing qualities.

(a) C100-V1.0-SP0.75	(b) C100-V1.0-SP1.0	(c) C100-V1.0-SP1.25

The Mix IDs describe the proportion of cement (C), VMA (V), and superplasticizer (SP) for each test.

Figure 3.3. Effects of superplasticizer on the 3D printing by syringe

Compared to the C100-V1.0-SP0.5, Figure 3.3a shows that the layers could not hold their shape right after extrusion, and the bottom layers started to widen. As the dosage of superplasticizer increased, it was easier to extrude the mixtures through the syringe, since the superplasticizer enhanced the flowability of the mixtures. However, the extruded layers could not hold their shape and resist the weight of the following deposited layers, and it led to collapse. Although Figure 3.3c shows more deposited layers, it collapsed inside, such that a larger number of layers seemed to be stacked.

In order to improve the shape stability of the mixtures, 2.5% of the cement was replaced by silica fume. Figure 3.4 shows the effects of chemical admixtures (VMA and superplasticizer) on the printing qualities of mixtures with silica fume.

(a) C97.5-SF2.5-V0.5-SP1.0	(b) C97.5-SF2.5-V1.0-SP1.0	(c) C97.5-SF2.5-V1.0-SP1.25

The Mix IDs describe the proportion of cement (C), silica fume (SF), VMA (V), and superplasticizer (SP) for each test.

Figure 3.4. Effects of chemical admixtures on the printing qualities of mixtures with silica fume

Compared to the C100-V1.0-SP1.0 test in Figure 3.3b, the C97.5-SF2.5-V1.0-SP1.0 sample in Figure 3.4b shows the usage of 2.5% silica fume significantly enhanced the buildability (shape stability). However, when the dosage of superplasticizer increased from 1.0% to 1.25%, the shape stability of the printed layers decreased, and the total number of deposited layers also decreased due to the wideness at the bottom layers.

During the printing process, one of the biggest problems was pop outs, and several samples demonstrated this problem as shown in Figure 3.5.

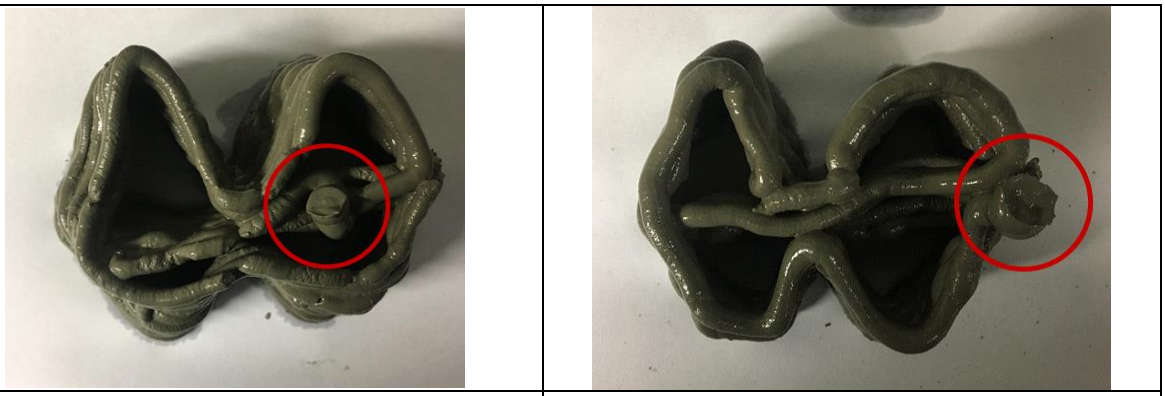

(a) C100-V0.5-SP0.5 (b) C100-V1.0-SP0.5

The Mix IDs describe the proportion of cement (C), VMA (V), and superplasticizer (SP) for each test.

Figure 3.5. Pop outs by air bubbles in the syringe

This defect happened frequently when air bubbles were created in the syringe. The entrapped air bubbles in the syringe came out of the nozzle, and it damaged the printed layers and discontinued the printing process. As discussed later, a similar problem also occurred when a commercial 3D printer was used for printing.

3.5 Summary

In this chapter, it was confirmed that the usage of VMA and superplasticizer had great impacts on printability. The VMA enhanced the viscosity of paste printing mixtures. However, it eventually decreased extrudability if the dosage was too high. Conversely, the superplasticizer increased the flowability and extrudability. However, if the dosage of superplasticizer was too high, the printed layers could not hold their shape and were deformed by the weight of subsequent deposited layers. Those test results indicated that it is essential to balance the dosage of materials to have proper flowability, extrudability, and printability.

In addition, it was observed during experiments that air bubbles came out of the nozzle and broke the layers. It is possible that air bubbles were created when the mixtures were placed into the syringe and came out of the nozzle due to the extrusion. This problem would be handled with suitable methods in the future tests.

4. PRINTER SELECTION AND PRINTING PARAMETER STUDY

4.1 Introduction of 3D Printer

A 3D pottery printer (3D plotter 7) was selected and used to print clay and concrete in this study, and it was selected to achieve a balance between its functionality and cost. Figure 4.1 shows photographs of the printer.

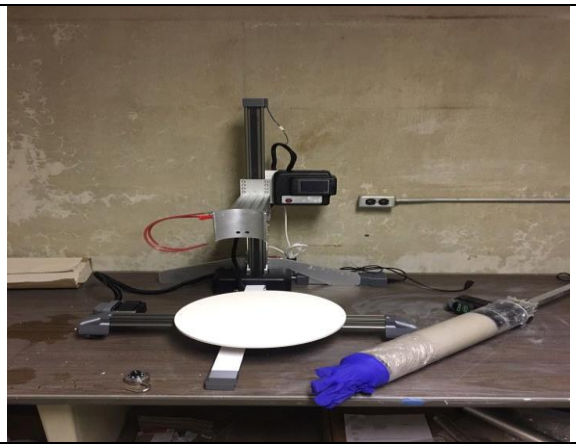

(a) 3D printer without mounting extruder

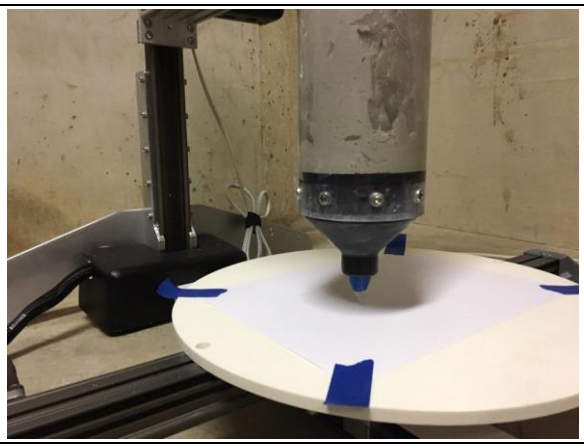

(b) 3D printer with mounting extruder

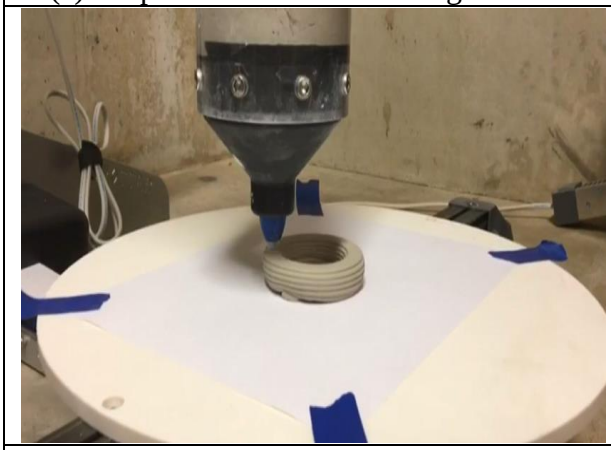

(c) 3D printing process

(d) Interface of 3D printer

Figure 4.1. 3D printer used in this study

The plotter had dimensions of 73.66 cm (wide), 81.28 cm (long), and 91.44 cm (high), and the maximum height is 195.5 cm when the extruder is fully extended. A platform moves along an x- and y-axis, and an extruder moves along a z-axis. An important feature of the printer is that users can control the extrusion and printing speed by using the interface shown in Figure 4.1d.

4.2 Printing Parameter Study

4.2.1 Overview

Before printing concrete, clay printing was conducted to get familiar with the new 3D printer. In addition to the operation, clay possesses less time-dependent behavior than concrete, since concrete sets significantly faster than clay. The tests with clay indicate that the printer is easy to use and convenient to control the overall printing process and investigate the effects of the printing parameters by conducting actual printing processes without wasting materials.

4.2.2 Materials

A commercial pottery clay (PRAI 3D) was used in this study, and its physical and chemical properties are presented in Table 4.1.

Table 4.1. Physical and chemical properties of clay

	Water content (%)	**Plasticity (IP Atterberg)**	**Carbonate content (%)**	**Drying shrinkage (%)**	**Porosity at Cone 10**
Clay	25.42	16	0	8.5	0

4.2.2 Printing Parameters

Among many printing parameters including printing speed, extrusion speed, infill rates, nozzle size and shape, printer type, stand-off distance, etc., two printing parameters (printing speed and extrusion speed) were selected for testing a variety of settings, and the other parameters were fixed in order to assess the effects of those specific printing parameters on the printing qualities. Table 4.2 shows the detailed printing parameters.

Table 4.2. Printing parameters for clay printing

Mix ID	**Printing speed (mm/s)**	**Extrusion speed (mm/s)**	**Nozzle diameter (mm)**	**Infill rate (%)**	**Layer thickness (mm)**	**Stand-off distance (mm)**
P30-E90	30	90	5	0	1.6	1.6
P60-E90	60					
P90-E90	90					
P60-E45	60	45				
P60-E135		135				

Default values for printing and extrusion speed were set at 60 and 90 mm/s, respectively. The Mix IDs describe the differing printing speeds (P), mm/s, and extrusion speeds (E), mm/s.

Three different printing speeds (30, 60, and 90 mm/s) and extrusion speeds (45, 90, and 135 mm/s) were set, respectively. A circular nozzle was used, and its diameter was 5 mm. Layer thickness and stand-off distance were set at 1.6 mm. Total printing time was limited to 1 min in order to use the same batch material to print three objects using three different printing speeds.

In addition to the effects of printing and extrusion speed on the printing qualities, infill rate was also selected for further study. Three different infill rates (0%, 60%, and 80%) were set, and the other parameters were fixed. Layer thickness and stand-off distance were set to 2 mm (Table 4.3).

Table 4.3. Printing parameters for clay printing

Mix ID	Infill rate (%)	Printing speed (mm/s)	Extrusion speed (mm/s)	Nozzle diameter (mm)	Layer thickness (mm)	Stand-off distance (mm)
IR0	0	30	38.5	5	2	2
IR60	60					
IR80	80					

The Mix IDs describe the varying infill rates (IR).

As shown in Figure 4.2b, a cylindrical object, with the dimensions of 40 mm in height and 80 mm in diameter, was printed with different infill rates.

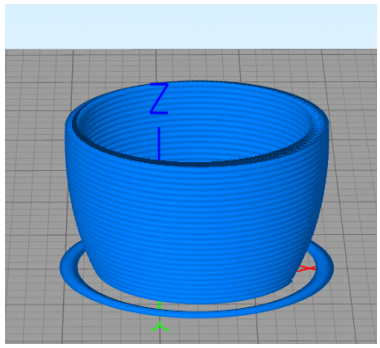

(a) 3D modeling for effects of printing speed and extrusion speed

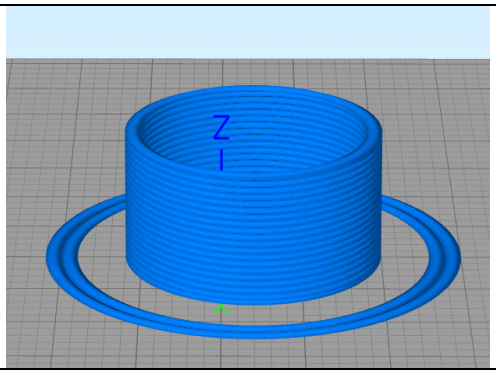

(a) 3D modeling for effects of infill rates

Figure 4.2. 3D modeling images

4.2.3 Printing Procedure and Test Methods

Clay was manually poured into the extruder and it was mounted on the printer shown in Figure 4.1. Before starting to print an object, initial layers were printed to check the extrudability of clay. After confirming the extrudability, the object printing process started based on the printing parameters set.

After finishing printing, layer width was measured by a ruler three times, and the average value was used as a test result. In addition, the overall shape of the printed objects was inspected visually.

4.2.4 Test Results

Figure 4.3 shows the effects of different printing speeds on the printing qualities.

Side view	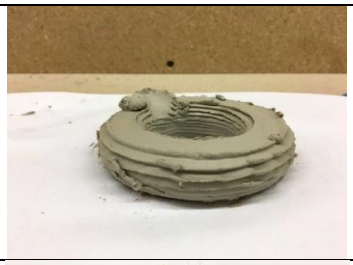		
Top view			
	(a) P30-E90	(b) P60-E90	(c) P90-E90

The Mix IDs describe the differing printing speeds (P), mm/s, and extrusion speeds (E), mm/s.

Figure 4.3. Effects of different printing speeds on the printing qualities

As printing speed increased from 30 mm/s to 90 mm/s, the height of the printed objects increased, since the printer head moved faster, and the extruder extruded more clay in the given time. Also, the layer width also increased as shown in Figures 4.3 and 4.5. This was because more clay was extruded than the setting, and as the number of printed layers increased, the amount of over-extruded clay also increased leading to the wider layer width.

Figure 4.4 illustrates the effect of different extrusion speeds on the printing qualities.

Side view			
Top view			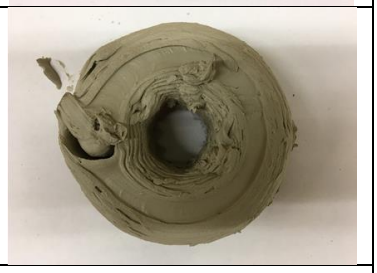
	(a) P60-E45	(b) P60-E90	(c) P60-E135

The Mix IDs describe the differing printing speeds (P), mm/s, and extrusion speeds (E), mm/s.

Figure 4.4. Effects of different extrusion speeds on the printing qualities

As the extrusion speed increased from 45.8 mm/s to 137.5 mm/s, the layer width was significantly increased, as shown in Figures 4.4 and 4.5. Also, the height of printed samples increased with increased extrusion speed. In addition to the geometry, the printing qualities of the objects' surface decreased as extrusion speed increased. It's possible this is because as the extrusion speed increased, excessive clay was extruded, which led to increased layer geometries (width and height) and poor printing qualities. Figure 4.5 shows the effects of printing and extrusion speed on the layer width.

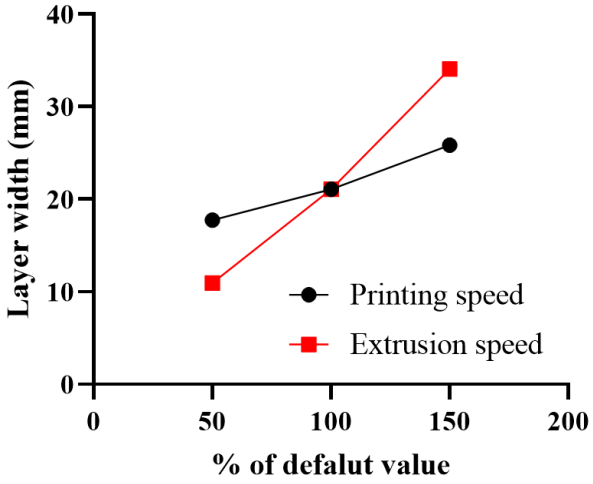

Figure 4.5. Effects of printing speed and extrusion speed on the layer width

It was found that both printing and extrusion speed affected the layer width, and the extrusion speed had more impact on the geometry of the printed objects than the printing speed. This result indicated that the combination of printing and extrusion speed was essential to print objects. As

shown in Figure 4.4a, the object printed with 60 mm/s printing speed and 45 mm/s extrusion speed was considered as the best printed sample. When the extrusion or printing speed changed, the overall printing quality deteriorated.

Figure 4.6 shows the effects of infill rates on the printing qualities.

Side view			
Top view		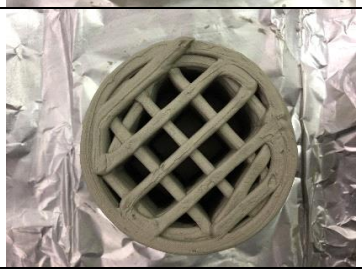	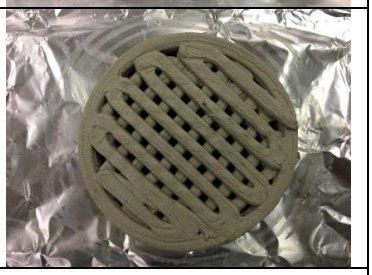
	(a) IR0	(b) IR60	(c) IR80

Mix IDs describe the varying infill rates (IR)

Figure 4.6. Effects of infill rates on the printing qualities

When the infill rate was set at 0%, there was no extruded clay in the printed sample, which looked like a hollow column. However, as the infill rate increased, the inside of the printed samples was filled with clay. This indicated that infill rate directly affected the density of the printed samples, and the infill rate should be set at 100% in order to print a solid column.

There were some problems during the printing process, which also had been noticed in the initial trial tests with the syringe. Air bubbles were found in several spots such as in the middle of printed layers and in the extruder. When the size of the air bubble was small, there was no significant defect in the printing qualities as shown in Figure 4.7a.

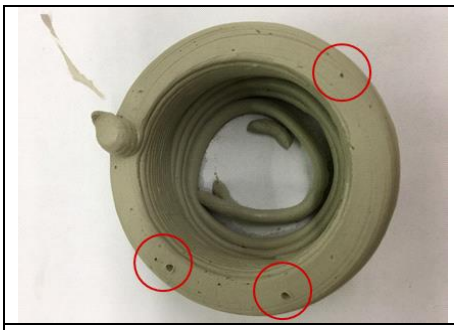

(a) Small air bubbles

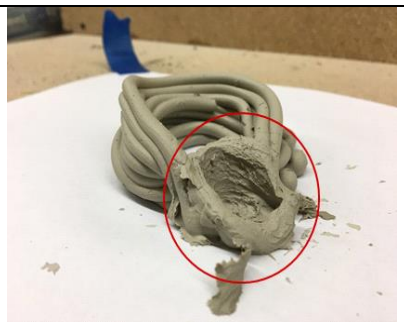

(b) Big air bubbles

Figure 4.7. Problems during clay printing process

However, when the size was big enough, the air bubble popped out of the printer nozzle and destroyed the printed layers as shown in Figure 4.7b. These results indicated that the ability to control the creation of air bubbles was as important as the printing parameters.

4.3 Summary

In this chapter, the printing parameters were investigated, and the research team found those settings significantly affected the printing qualities including the geometry of printed objects. Among various printing parameters, printing speed and extrusion speed were selected to test various rates, and other parameters were fixed. It was observed that layer width widened with increased printing and extrusion speed, and extrusion speed affected the layer width more than printing speed Therefore, it is essential to find the best combination of printing parameters. In addition to the printing parameters, it was also found that infill rates could affect the printing qualities. As the infill rates increased, the density of objects increased since the inside space was filled with clay.

As mentioned in the previous chapter, air bubbles were observed during clay printing. Normally, clay has higher viscosity than concrete, and it was more difficult to eliminate air bubbles when clay was poured into the extruder. Thus, bigger bubbles were created in the extruder, and they destroyed the printed layers when they came out of the nozzle. The findings indicated that suitable methods to eliminate air bubbles should be considered when concrete is used to print.

5. 3D PRINTING CONCRETE MIX DESIGN AND OPTIMIZATION

From the initial trial tests as described in Chapter 3, Figure 3.4b indicates that Mix C97.5-SF2.5-V1.0-SP1.0, which is made with 97.5% portland cement, 2.5% silica fume, 1% VMA, and 1% superplasticizer, showed good performance in terms of extrudability and buildability for 3D printing. However, when the 3D pottery printer was used, this mix proportion had to be re-adjusted to be able to be easily placed in the printer, extruded out consistently, and hold its shape during and after printing. VMA and superplasticizer were used for the flowability adjustment. However, it was found that uniformity in the printable mixtures was difficult to achieve as slight differences in the mixture's flowability and stiffening behavior could lead to quite different properties of printing concrete.

In addition to VMA and superplasticizer, an accelerator appeared necessary for a mixture to develop stiffness rapidly to carry the weight of subsequent concrete layers without distortion. To simplify the mix design procedure, the researchers of this project decided to use a highly flowable, rapid-set grout as a partial cement replacement to adjust the extrudability and printability of the 3D printing concrete mixtures, instead of trying various admixtures (VMA, superplasticizer, and accelerator/retarder). The results from the use of a grout to develop 3D printable concrete mixtures are presented in the following sections.

5.1 Materials

Cementitious materials used in this study included Type I/II portland cement, silica fume, and a highly flowable, rapid-set grout. The chemical composition of portland cement and silica fume are presented in Table 3.2. The grout was a commercial product from China, which was used in a previous Iowa Highway Research Board (IHRB) research project (TR-708B). It consisted of calcium sulfoaluminate cement, fine sand, and various additives. Fluidity and setting time of grout are presented in Table 5.1, and the strength development of grout is shown in Figure 5.1.

Table 5.1. Fluidity and setting time of grout

	Fluidity (s)		Setting time (min)	
Material	**0 min**	**30 min**	**Initial**	**Final**
Grout	15	18	120	150

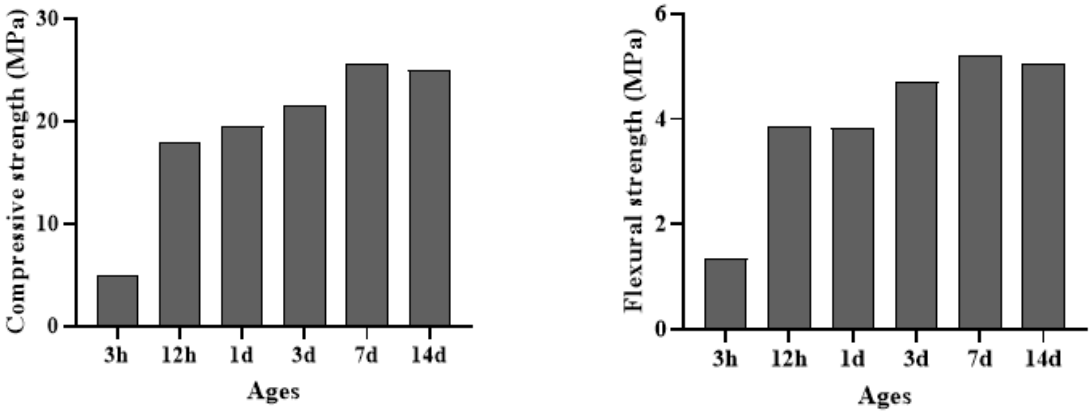

(a) Compressive strength (b) Flexural strength

Wang and Hong 2019, Institute for Transportation

Figure 5.1. Strength development of grout used

Detailed information on this grout can be found in Wang and Hong (2019) and Hong et al. (2019). A small amount of additional VMA and superplasticizer were also used to adjust the segregation resistance and flowability of the 3D printing mortar.

5.2 Mix Proportions and Mixing Procedure

Different types and dosages of materials were used to develop 3D printable concrete/mortar mixtures, and the mix proportions studied are presented in Table 5.2.

Table 5.2. Mix proportion for 3D printable concrete

Mix ID	w/b	Cement	Silica fume	Grout	VMA (binder %)	Superplasticizer (binder %)
V0-SP1.00	0.30	97.5	2.5	-	-	1.00
V1.00-SP1.00	0.30	97.5	2.5	-	1.00	1.00
V1.00-SP1.25	0.30	97.5	2.5	-	1.00	1.25
V1.25-SP1.25	0.32	97.5	2.5	-	1.25	1.25
V1.50-SP1.25	0.32	97.5	2.5	-	1.50	1.25
V1.75-SP1.25	0.32	97.5	2.5	-	1.75	1.25
G20-SP1.25	0.32	77.5	2.5	20	1.50	1.25
G20-SP1.25	0.32	67.5	2.5	30	1.50	1.25
G30-SP0.30	0.32	67.5	2.5	30	1.50	0.30
0.28-G20	0.28	77.5	2.5	20	1.50	-
0.30-G20	0.30	77.5	2.5	20	1.50	-
0.32-G30	0.32	77.5	2.5	20	1.50	-

The sum of binder (cement+silica fume+grout) is 100. The Mix IDs describe the proportion of VMA (V), superplasticizer (SP), grout (G), and w/b for each test.

All mixtures were fabricated at the Portland Cement Concrete Pavement and Materials Research Laboratory (PCC Lab) at Iowa State University (ISU). For uniform dispersion, raw materials were first dry-mixed for 5 min using a Hobart mixer. Then, half the water and all of the superplasticizer were added into the mixture and mixed for 1 min. Next, the remaining half of the water and all of the VMA were added into the mixture and mixed for another 1 min. Next, the mixture rested for 1 min while the residuals were scraped off the surfaces of the mixing blade and bowl. Finally, the mixture was mixed for another 3 min. Thus, the total mixing time was 11 min including 1 min of rest.

5.3 Printing Parameters and Procedure

A cylindrical object (60 mm in diameter and 120 mm in height) was designed by AutoCAD and saved in a structure file (.str). Then, using the Simplify3D software, which is a slicer program, the object was sliced into several layers shown in Figure 5.2.

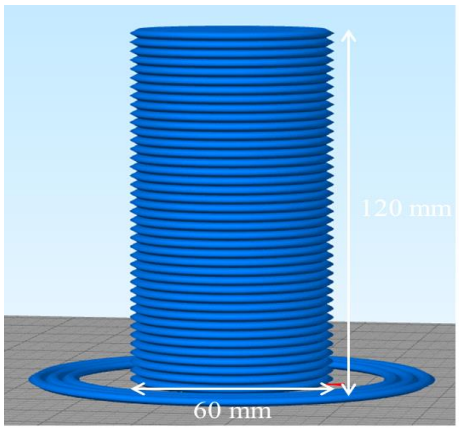

Figure 5.2. 3D modeling image

Detailed printing parameters used in this study are presented in Table 5.3.

Table 5.3. Printing parameters for concrete printing

	Printing speed (mm/s)	Extrusion speed (mm/s)	Nozzle diameter (mm)	Layer thickness (mm)	Stand-off distance (mm)	Mixing time (minutes)	Starting time (minutes)
Concrete printing	12	61.5	6.5	3	3	11	45

After completion of the printing process, the printed objects were immediately covered by a plastic cover and a plastic sheet for 6 hours to prevent water evaporation (Figure 5.3).

Figure 5.3. Curing method

Then, they were moved into a standard curing room (73.4±3.5°F and ≥95% RH) and kept there until testing.

5.4 Evaluation Methods

As mentioned previously in Table 2.1, several properties are critical for a 3D printable concrete mixture, and they are (1) flowability, (2) extrudability, and (3) buildability, and (4) printability.

In this project, flowability of 3D printable mortar mixtures was assessed by flow table tests and visual inspection. The flow table tests were used according to ASTM 1437, and detailed information on the tests will be explained in the next chapter. The visual inspection was performed to see and feel whether mixtures were easily poured into the extruder of the printer.

Extrudability was evaluated by observing the (1) continuity and (2) uniformity of the extruded filaments of a mixture from the start to end of printing. Some mixtures had rapid stiffening behavior with printing time and led to a blockage at the nozzle tip, thus showing poor continuity of printed filaments. Under- or over-extrusion would cause non-uniform filaments to come out from the nozzle, and large air bubbles entrapped in the mixture could cause pop outs, thus showing poor uniformity.

Buildability was estimated by inspecting slump and distortion of freshly printed objects. When the printing mortar did not have enough stiffness or strength to hold the shapes and carry the weight of the layers deposited above, the printed object would slump, deform, or collapse. When any of these occur, the mixture was considered as having unsuitable buildability.

Printability was assessed based on the overall result of flowability, extrudability, and buildability. If one of those properties was not fulfilled, an object was considered as lacking in printability.

5.5 Test Results

Figure 5.4 shows the effects of the VMA and superplasticizer on the concrete printing.

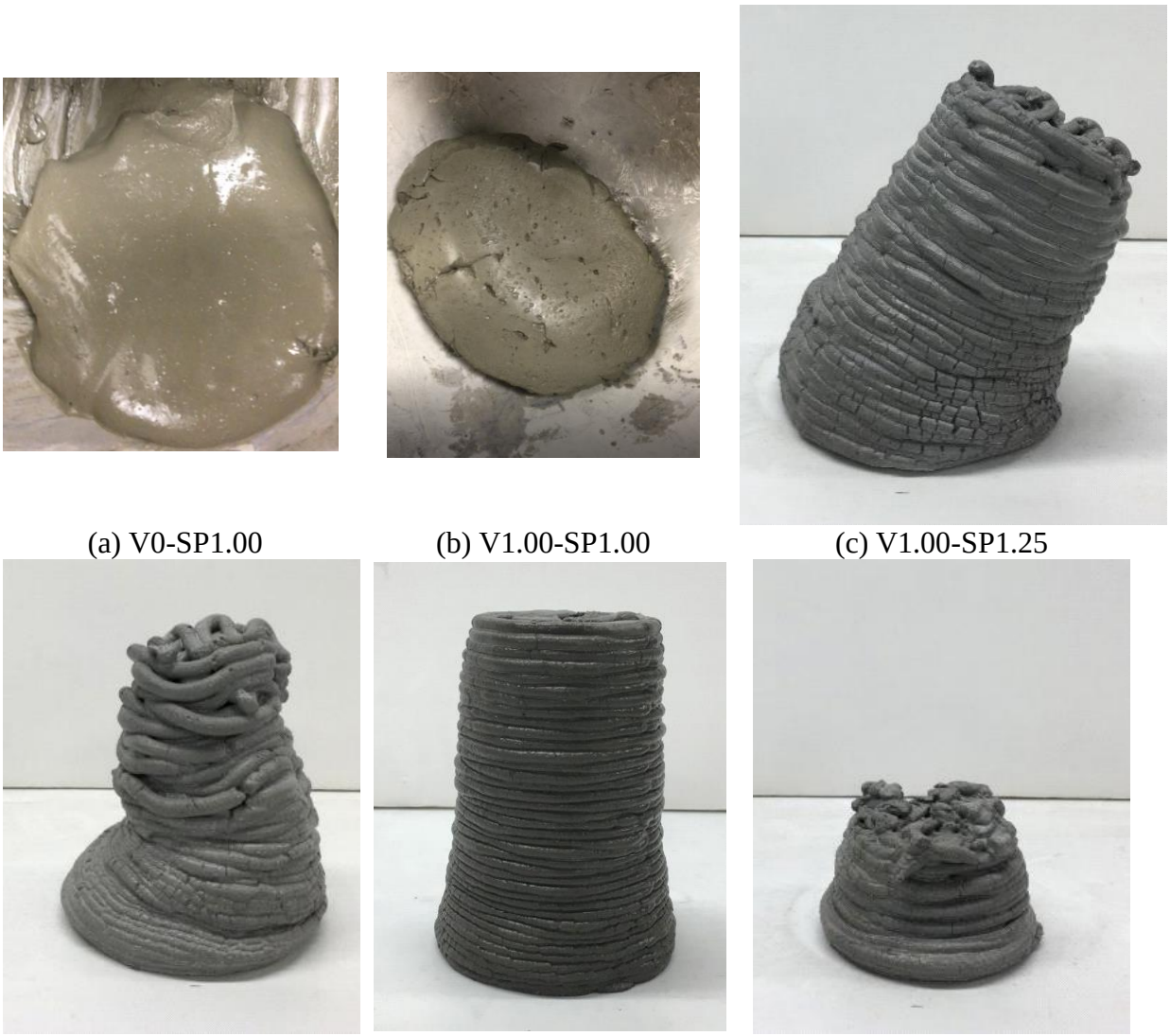

(a) V0-SP1.00 (b) V1.00-SP1.00 (c) V1.00-SP1.25

(d) V1.25-SP1.25 (e) V1.50-SP1.25 (f) V1.75-SP1.25

The Mix IDs describe the proportion of VMA (V) and superplasticizer (SP) for each test.

Figure 5.4. Effects of VMA and superplasticizer on concrete printing

In the case of V0-SP1.00 and V1.00-SP1.00, the objects could not be printed because the material was too flowable and too thick, respectively. When V1.00-SP1.25 was used to print, at the beginning, the object was printed. However, as time passed, the bottom layers started to collapse, and the overall shape was eventually distorted. Therefore, the addition of more VMAs was required, and 1.25%, 1.50%, and 1.75% of the VMA was incorporated in the mixtures (Figure 5.4d, e, and f). If 1.75% of the VMA was added in the mix design, the mixture was too thick to be extruded from the nozzle, and extrudability decreased. Even though V1.50-SP1.25 seemed to be well-printed, the bottom layers widened, and the object ended up a bit slumped.

Figure 5.5 shows the effects of grout and superplasticizer on the printing qualities of the 3D printed concrete objects.

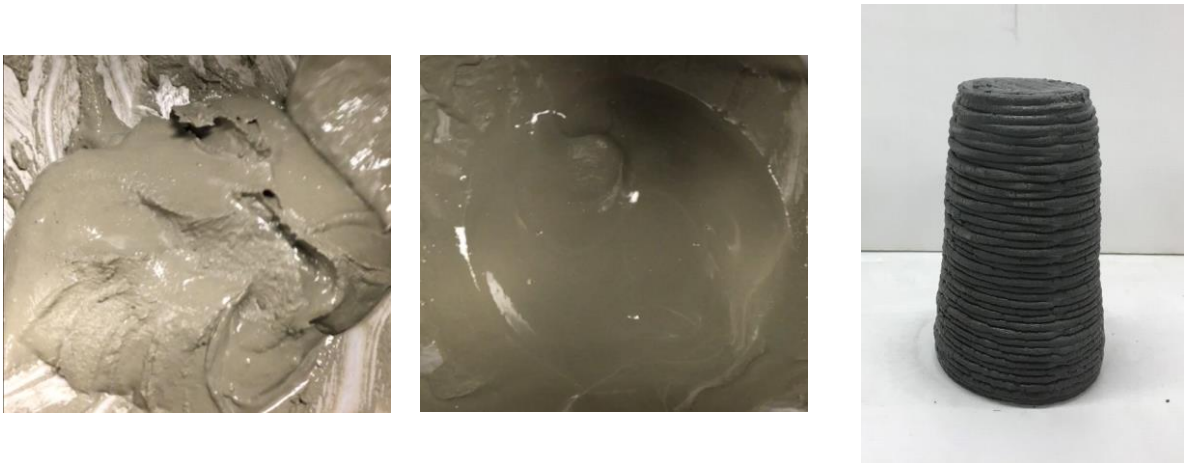

(a) G20-SP1.25 (b) G30-SP1.25 (c) G30-SP0.3

The Mix IDs describe the proportion of grout (G) and superplasticizer (SP) for each test.

Figure 5.5. Effects of the grout and superplasticizer on the concrete printing

Since grout includes powder-form superplasticizer, as the replacement ratio of grout increased, the mixtures became flowable. Therefore, when the dosage of superplasticizer decreased from 1.25% to 0.3%, with 30% of grout, the cylindrical object (Figure 5.5c) was able to be printed but with slump.

Figure 5.6 shows the effects of the w/b ratio on the printing qualities.

(a) 0.28-G20 (b) 0.30-G20 (c) 0.32-G20

The Mix IDs describe the w/b ratio and proportion of grout (G) for each test.

Figure 5.6. Effects of w/b on the concrete printing

As the ratio increased, the mixtures became flowable, and 0.32-G20 offered the best mix proportions. Although 0.30-G20 seemed to be well-printed, extrudability decreased as time passed, and the last printed layer was not smoothly extruded, leading to the discontinuity.

Figure 5.7 shows the effects of printing speed on the printing qualities when all the printed objects were printed with 0.32-G20, which was the best mix design based on the overall shape.

(a) 12 mm/s (b) 24 mm/s (c) 12+24 mm/s

Figure 5.7. Effects of printing speed on the printing qualities

As the printing speed doubled, the bottom layers became wide, and the overall shape was distorted even though the same mixture was used (Figure 5.7b). It's possible the printed layers were not able to harden due to the increased printing speed, and the layers could not hold the weight of the subsequent layers. When two different printing speeds (12 and 24 mm/s) were used, the overall shape was better than only the higher printing speed (24 mm/s); however, distortion at the bottom layers was still observed.

Several defects were identified during 3D concrete printing, and they were (a) air bubble pop outs, (b) discontinuity, (c) slumping, and (d) cracking (Figure 5.8).

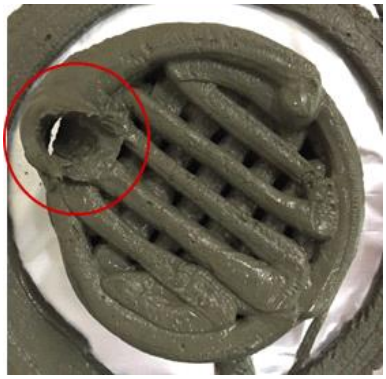

(a) Air bubble pop outs

(b) Discontinuity

(c) Slump

(d) Cracks

Figure 5.8. Problems during concrete printing process

Air bubbles were a major problem during the printing process. Under extrusion pressure, air bubbles often popped out (Figure 5.8a), and they destroyed printed layers, or led to discontinuity of printed layers. Air bubble pop outs were mostly observed in the mixtures having relatively high flowability. When the mixtures had relatively low flowability, discontinuity of filaments was often observed (Figure 5.8b). Slump of objects occurred when the flowability of the mixture was slightly higher, and the rate of stiffening of the mixture was a little slower. Visible slump of printed objects indicates impaired buildability (Figure 5.8c). In order to improve buildability, most 3D printable concrete mixtures were designed to have a low w/b, which often led to a high potential for plastic shrinkage cracking (Figure 5.8d). Prompt curing was essential to reduce slump as well as plastic shrinkage cracks, for which all printed objects were covered with a plastic sheet immediately after being printed and before being moved into a standard curing room.

6. MIXTURE CHARACTERIZATION AND PROPERTIES OF 3D PRINTED PRODUCTS

6.1 Overview

After the 3D printable concrete mix design tests, it was confirmed that use of grout to replace some cement facilitated rapid development of a mixture's stiffness and brought about better buildability. Therefore, different replacement ratios of grout were estimated by printing a cylindrical object. Then, the mechanical properties of a printed sample with the best mix proportion were assessed.

6.2 Materials, Mix Proportions, and Procedure

As binder materials, portland cement, silica fume, and grout were used to prepare 3D printable concrete. In addition, VMA and superplasticizer were added into the mixtures to enhance the segregation resistance and flowability. Detailed information on the materials including chemical composition and properties were presented previously in Tables 3.2 and 5.1 and Figure 5.1.

To find the best mix proportion, the weight of a percentage of cement was replaced by grout (at rates of 0%, 10%, 20%, and 30%); Table 6.1 shows the mix proportions used in the tests.

Table 6.1. Mix proportion with different replacement ratio of grout

Mix ID	w/b	Cement	Silica fume	Grout	VMA (binder %)
0.32-G00	0.32	97.5	2.5	0	1.5
0.32-G10		87.5		10	
0.32-G20		77.5		20	
0.32-G30		67.5		30	

The sum of binder (cement+silica fume+grout) is 100% (by weight). The Mix IDs describe the w/b ratio and proportion of grout (G) for each test.

The mixing procedure was based on the one described in the previous chapter.

6.3 Printing Parameters and Procedure

The printing parameters and procedure were based on tests from the previous chapter.

6.4 Test Methods

6.4.1 Fresh Concrete Properties

Flow table tests were used to measure the flowability of the mixtures based on ASTM C1437. A conical cone was filled with a mixture, the spread diameters were measured at three different diameters after the cone was lifted up, and the flow table was dropped 25 times. The average value of spread diameters was used as the flowability result in this study.

In addition, the changes in flowability with increased time were assessed by measuring the spread diameters at 0, 20, 40, and 60 min after the mortar was mixed. The printing of the designed object could start approximately 40 min after the mortar was mixed, since the preparation for 3D printing, including feeding mortars into the extruder, printer setup, and pre-printing, took approximately 40 min. Moreover, the printing process took approximately 20 min to complete the cylindrical object.

Extrudability and printability were assessed based on visual observations.

6.4.2 Mechanical Properties

Due to the unique property of the 3D printed object, which is its anisotropic behavior, the mechanical properties were closely related to the relationship between the printing and loading direction. Therefore, in this study, two different configurations of prisms were printed to prepare cubic and slab samples for compressive and flexural strength tests shown in Figure 6.1.

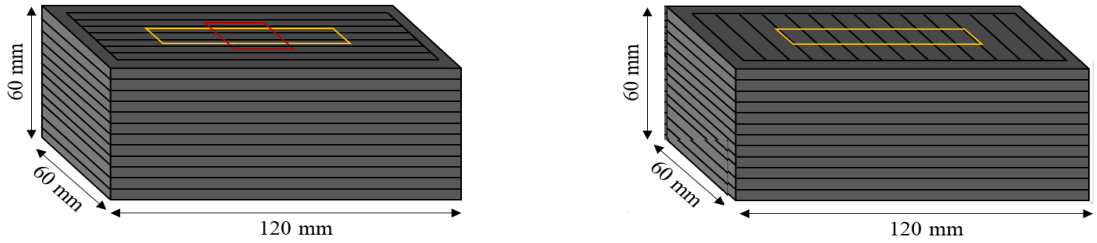

(a) Prisms with two different printing directions: red and yellow squares represent cutting area of samples for compressive and flexural strength, respectively

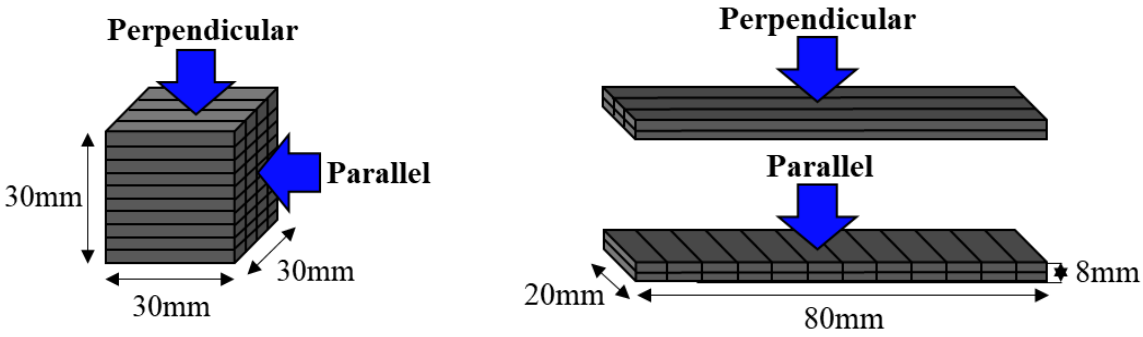

(b) Cubic sample for compression test (c) Slab samples for flexural h test

Figure 6.1. Sample preparation for mechanical properties

The cut cubic samples and slab samples could be loaded in two different loading directions, perpendicular and parallel to the printing direction.

The mechanical properties were assessed at different testing ages (7 and 28 days of curing), and Figure 6.2 shows the cut samples at 28 days.

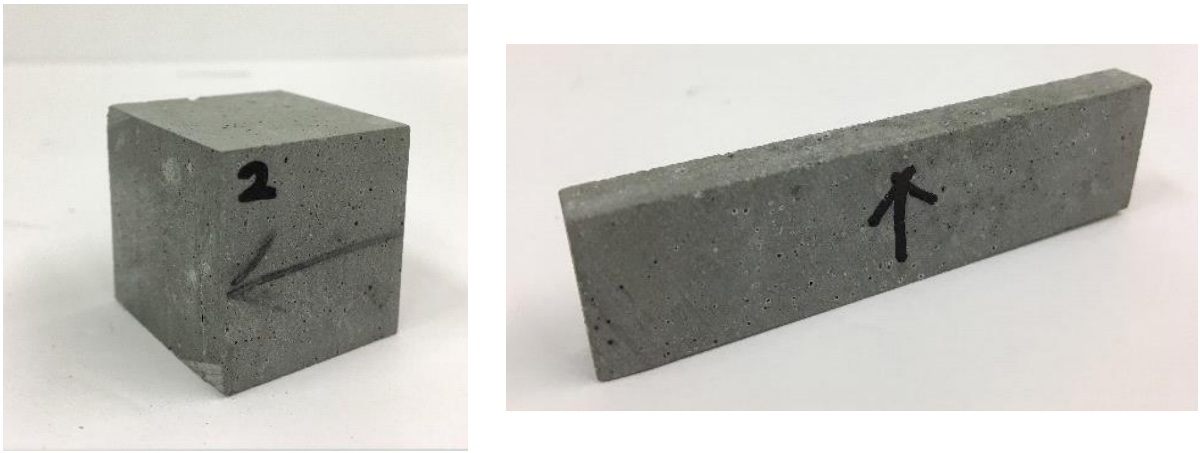

Figure 6.2. Cut samples for mechanical properties

In addition to the cut samples from the printed samples, mold-cast samples were prepared for a comparison. The compressive strength and flexural strength were tested based on ASTM C109

and ASTM C293, respectively. For each test, five cut samples were tested, and the average value was used as the final result.

6.5 Test Results

6.5.1 Flowability

Table 6.2 shows the flow table test results of mortar mixtures performed at 0, 40, and 60 min after completion of mixing.

Table 6.2. Results from flow table test

	Final flow diameter (mm) at different rest time (minutes)				
Mix ID	**0 min**	**40 min**	**60 min**	**0–40 min**	**40–60 min**
0.32-G00	203	197	192	6	5
0.32-G10	190	174	170	16	4
0.32-G20	220	182	176	38	6
0.32-G30	244	207	200	37	7

All mixes had a w/b of 0.32 but different amount of grout (G) replacement for cement.

The data in the table were the final flow spread (at 25 drops) values, because after 40 min rest, the initial and final flow spread values were very close as some pastes were about to set. Therefore, only the final flow spread results are presented here. The flowability at 0 min rest indicates the flowability of the tested mixture at the time of being placed into the 3D printer. The higher this flow is, the easier the mixture is placed. The flowability at 40 min rest presents the flowability of the tested mixture at the beginning of the extrusion or printing, which is related to extrudability and buildability. If this flow is too low, the mixture will be difficult to extrude. If it is too high, the filament will not hold its shape. The flowability at 60 min signified the flowability of the tested mixture at the end of the extrusion or printing.

In addition to the flowability value at each of the specified rest times, which is essential, the differences (reductions) in flowability from 0 to 40 min and from 40 to 60 min rest times are also important. A large flowability reduction from 0 to 40 min rest times suggests that the mixture would be easily placed into the printer, and the filaments could be well printed out with a uniform shape. The flowability reduction from 40 to 60 min rest times is related to open time, the period during which the mixture is printable. The larger this reduction, the shorter the open time of the mixture.

It can be observed from Table 6.2 that with 0 min rest, the samples containing a higher amount of grout had a higher flowability. However, Mix 0.32-G10 (10% grout) showed a reduced flow than Mix 0.32-G0 (no grout). This is because the grout consisted of rapid-set CSA cement and dry-powder superplasticizer. At small dosages, the effect of CSA cement hydration, which reduced flow, exceeded the effect of the superplasticizer, which increased flow, thus reducing the overall flow of the mortar. After 40 min rest, the flowability of all mixtures decreased when compared with those at 0 min rest, due to cement hydration. Mix 0.32-G10 had the lowest flow

at 40 min rest among all mixtures studied, which was difficult to extrude from the nozzle. The rest of the mixes were able to be extruded from the nozzle, but those having a high flow at 40 and 60 min rest and a small flow reduction during 0-60 min rest, e.g., Mix 0.32-G0, were unable to hold the shape of extruded filaments and/or printed objects. As a result, only Mixes 0.32-G20 and 0.32-G30 were suitable for printing. Additional related discussions on extrudability and buildability are presented in the following section.

6.5.2 Extrudability and Buildability

As discussed previously, among the four mixes made with different amounts of grout, only Mixes 0.32-G20 and 0.32-G30 were able to be printed. Figure 6.3 illustrates the freshly printed object with Mixes 0.32-G20 and 0.32-G30.

(a) Mix 0.32-G20

(b) Mix 0.32-G30

The Mix IDs describe the w/b ratio and proportion of grout (G) for each test.

Figure 6.3. Buildability of printable mortars illustrated by the shape of printed objects

It can be observed that Mix 0.32-G20 had very close to the designed 3D model, and it indicated that it had a good printability. However, Mix 0.32-G30 showed slump and distortion. Because of the high flow values of Mix 0.32-G30 at 40 and 60 min rest, the object printed with Mix 0.32-G30 slumped under the weight of itself, having a larger diameter at the bottom and a non-uniform overall layer thickness. Because the slump occurred during printing, the layers were not deposited at the locations set by the 3D modeling tool, thus reflecting poor extrudability and buildability. Therefore, Mix 0.32-G20 was chosen for further study on the mechanical properties of 3D printing concrete (sections 6.5.3 and 6.5.4).

6.5.3 Compressive Strength

The samples used for mechanical tests (compressive and flexural strength) were all prepared from Mix 0.32-G20. The mechanical properties of the 3D printed samples were compared with those of mold-cast samples. Direct tension tests were also performed. However, due to the

limitations of sample size and testing equipment, as well as the brittle failure of the samples immediately after loading started, no measurements were able to be taken. Figure 6.4 shows photographs of the broken samples from the direct tension tests. Therefore, only compressive and flexural strength test results are presented in this report.

Figure 6.4. Failures during direct tension tests

Figure 6.5 shows the compressive strength test results of mold-cast and 3D printed samples at 7 and 28 days.

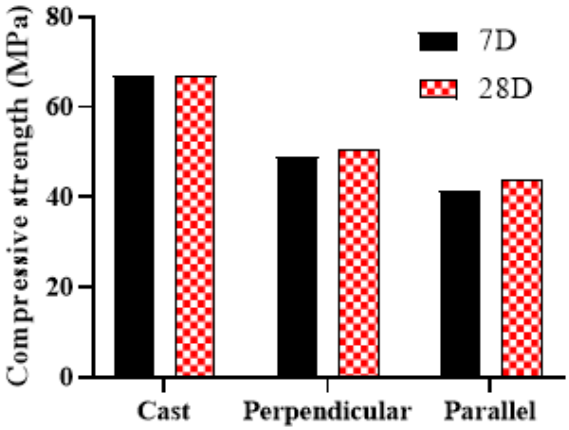

Figure 6.5. Compressive strength at 7 and 28 days

For the printed samples, load was applied to the direction perpendicular and parallel to the filaments of the samples to examine the anisotropic behavior of the 3D printed concrete.

It can be seen from the figure that the compressive strength of the cast samples was around 67 MPa, at 7 and 28 days, the highest among all samples tested. The reason for which there was little to no change in compressive strength from 7 to 28 days might be related to the CSA in grout. It has been reported that CSA cement showed strength loss at later ages due to the conversion of ettringite to less volumetric monosulfate, leading to increased porosity. Thus, the strength increase resulting from portland cement hydration was offset by the strength loss resulting from the phase transformation of CSA cement hydration products.

Figure 6.4 also shows that 3D printed samples had significantly lower strength than the cast sample at both 7 and 28 days. Most researchers believe that this is attributed to the weak bonds between the printed filaments of the printed samples. Several researchers have studied the bond properties of 3D printed concrete and proposed different methods to improve the bond strength (Marchment et al. 2019). In addition, the samples loaded in the direction perpendicular to printed filaments had a 28 day compressive strength of 50 MPa, about 17% lower than the mold-cast sample; while samples loaded in the direction parallel to printed filaments had a 28 day compressive strength of 44 MPa, about 27% lower than mold-cast sample. This clearly demonstrated the anisotropic behavior of 3D printing concrete.

Figure 6.6 illustrates the failure modes of these samples.

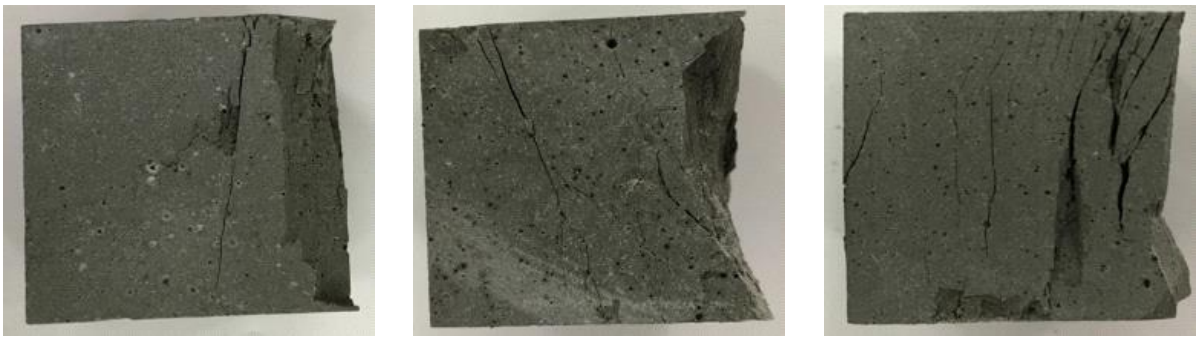

(a) Cast sample

(b) Sample loaded in the direction perpendicular to printed filaments

(c) Sample loaded in the direction parallel to printed filaments

Figure 6.6. Failure modes of samples under compression tested at 28 days

It can be seen from the figure that the mold-cast sample had a typical brittle failure shown by very few, nearly vertical cracks. The sample loaded in the direction perpendicular to printed filaments showed a major diagonal crack, across the cross section of many filaments of the sample, indicating that these filaments had a shear failure under the compressive load. Alternatively, the sample loaded in the direction parallel to printed filaments showed a larger number of vertical cracks than others, probably caused by the separation of the adjacent filaments. These vertical cracks were larger at the edges and finer at the center of the tested sample. This might be because the vertical filaments had less/no restraint at the edges of the sample, and they were easier to bend (or buckle) under the vertical compressive load. The bending deformation generated tensile stresses that separated the filaments and caused bond

failures or large cracks. At the center of the sample, individual filaments were difficult to bend due to the restraint supplied by adjacent filaments, thus causing small cracks.

6.5.4 Flexural Strength

Figure 6.7 shows the flexural strength test results of cast and printed samples at 7 and 28 days.

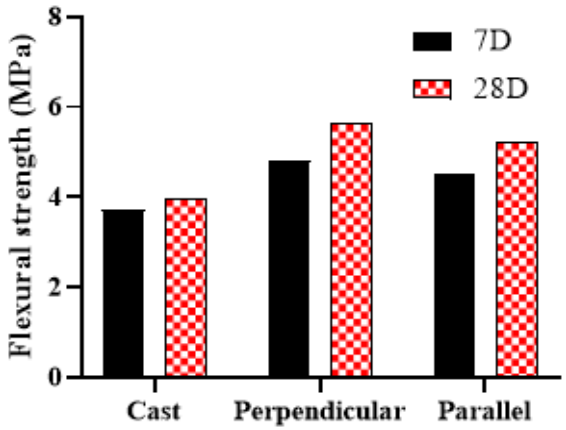

Figure 6.7. Flexural strength at 7 and 28 days

Different from the results of compressive strength, flexural strength of the printed samples was higher than that of the cast sample, regardless of interlayers between filaments and loading directions.

As seen in the figure, the flexural strength values of the cast samples were 3.8 MPa and 4.0 MPa at 7 and 28 days, respectively. For the samples loaded in the direction perpendicular to printed filaments, these strength values were 4.9 MPa and 5.7 MPa, about 29% and 45% higher than those of the mold-cast sample at 7 and 28 days, respectively. For the samples loaded in the direction parallel to printed filaments, these strength values were 4.6 MPa and 5.2 MPa, about 21% and 32% higher than those of the mold-cast sample at 7 and 28 days, respectively. Compared with compressive strength values, the differences in flexural strength values of the 3D printed samples loaded in different directions were much smaller, indicating less severe anisotropic behavior of 3D printing concrete under flexural loading.

The phenomenon that the 3D printed samples had higher flexural strength than mold-cast samples was also observed by other researchers (Marchment et al. 2019). One explanation is that during the printing process mortars were compacted and densified, and it led to a densified microstructure. More studies are necessary to verify this inference. However, little explanation could be made on why the 3D printed samples had higher flexural strength than cast samples when they were loaded parallel to the filaments. Further study on this subject is necessary.

The failure modes of the mold-cast and 3D printed beams are presented in Figure 6.8.

(a) Cast sample

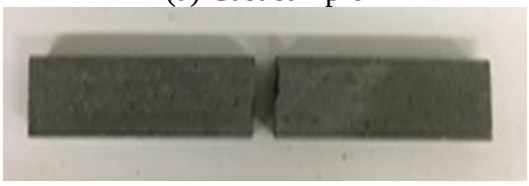

(b) Sample loaded perpendicular to printed filaments

(c) Sample loaded parallel to printed filaments

Figure 6.8. Failure modes of samples under flexural load tested at 28 days

It appears that all samples displayed a similar brittle failure. It should be noted that at 28 days, the ratio of flexural strength-to-compressive strength of the cast sample was about 6% for cast samples, while it was over 11% for the 3D printed samples in both loading directions. This implies that for a given concrete mixture, a component manufactured with a 3D printing process may have a higher cracking resistance than one manufactured with a conventional mold-cast process.

It should be noted that the mechanical behavior of 3D printing concrete depends upon not only the concrete materials, mix proportion, printing direction, and curing conditions but also printing parameters (e.g., extrusion and printing speeds), sample and filament sizes, open time, etc. Much more work needs to be done to have a better understanding of the overall mechanical behavior of 3D printing concrete.

7. OBJECT DESIGN AND QUALITY EVALUATION

7.1 Object Design

With clay and concrete, different shapes of objects were printed, and Figure 7.1 shows the objects printed using the 3D printer in this present study.

Cup

Small bottle

Rectangular

(a) Clay objects with different shapes

0% Infill

60% Infill

80% Infill

(b) Clay objects (80 mm × 40 mm cylinder) with different infill rates

60 mm × 120 mm cylinder

60 mm × 60 mm × 120 mm prism (Vertical)

60 mm × 120 mm × 60 mm prism (Horizontal)

(c) Concrete objects

Figure 7.1. Different objects printed with clay and concrete

Cup, bottle, and rectangular shapes were designed and printed with clay. In addition, different infill rates were used to print cylindrical objects to investigate their effects on the printed objects. After the printing parameter studies, concrete was used as an ink for 3D printing, and cylindrical and rectangular shapes were printed with concrete.

7.2 Printing Quality Evaluation

Although 3D printing quality attracts great attention, there is very limited information on how to evaluate the quality of 3D printed objects. The commonly used evaluation method is visual inspection. In order to compare the quality of the 3D printed concrete objects created in the present study with that of objects printed by other researchers, a qualitative ranking system based on visual inspection was developed in the present study.

Figure 7.2 illustrates the qualitative ranking system developed for evaluation of the printing qualities of 3D concrete printing, where 1 and 5 represent the best and worst printing qualities, respectively.

The 3D printed objects ranked 1 have smooth or uniform layers and those ranked 5 were not able to be evaluated due to the incapability to be printed. The images used in the ranking system were collected from various publications as labeled in the figure, and their citations can be found at the end of this report. Based on this ranking system, the samples printed with the best mortar mixtures used in the present study could be ranked as 2, since they showed quite uniform layers and only slightly rough surfaces.

In order to have a quantitative evaluation of the printing qualities, a 3D structured light scanning system (3D-SLSS) was applied to assess the printing qualities of the 3D printed clay samples (Wi et al. 2020). To conduct the analysis, a 3D-SLSS was used to scan the printed objects and create 3D images of the samples. The images then were sliced to generate a number of 2D plots, from which various parameters (e.g., sample total height, outer/inner diameter, layer thickness, layer width, and surface roughness) were measured with high accuracy. The quality of the printed objects can be evaluated by comparing the measurements of the printed samples with the designed values.

1- the best
5- unable to print

Our printed sample might be ranked as "**2**".

Rank	Description	Images
1	A printed object with smooth or uniform layers	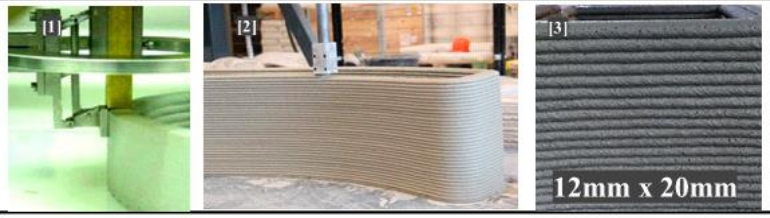
2	A printed object with rather uniform layers and a bit rough surface	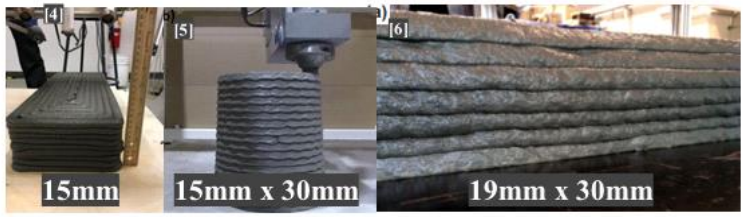
3	A printed object with rather uneven layers and rough surface	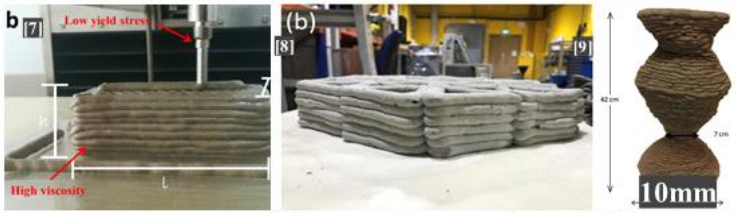
4	Not a printed object but a few built layers	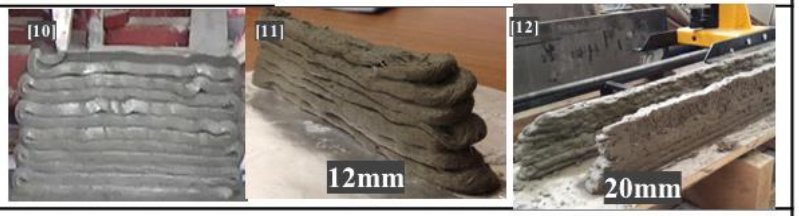
5	Not able to print	

Figure 7.2. Printing quality evaluation and comparison

Figure 7.3 shows photographs and 3D images of selected 3D printed clay samples.

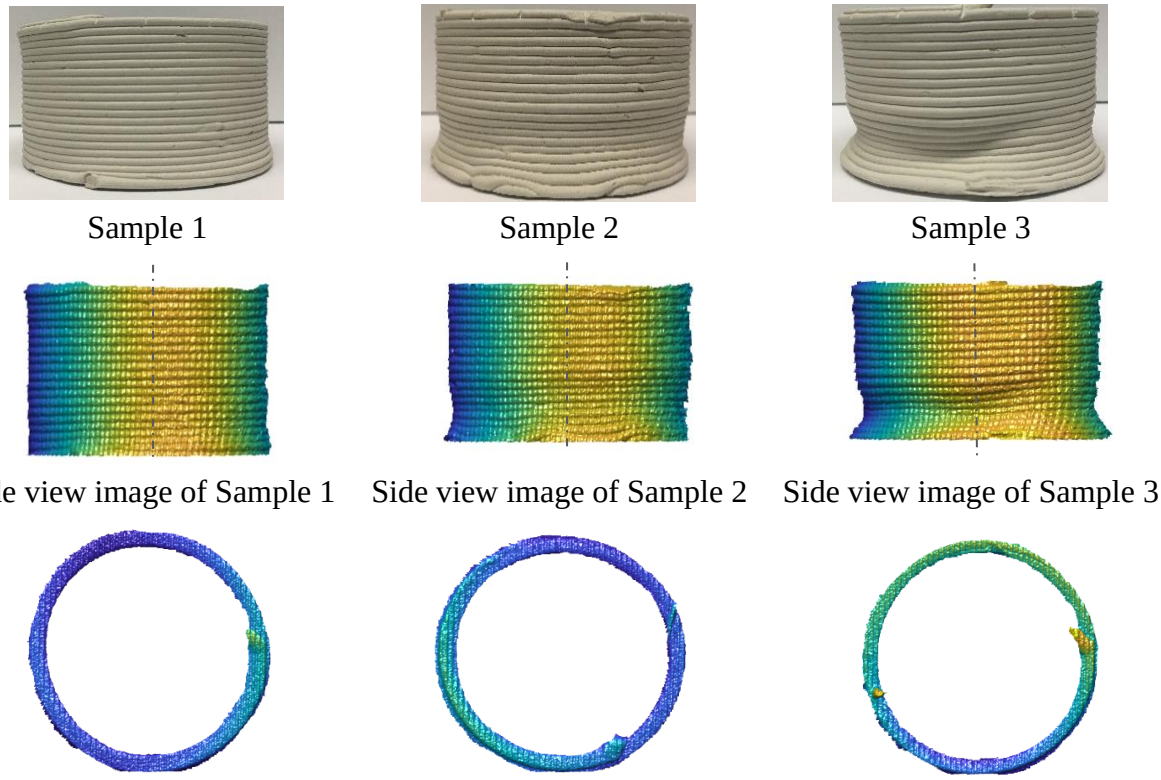

Figure 7.3. Photos and 3D-SLSS images of 3D printed clay samples

The designed dimensions of these hollow cylindrical samples were 80 mm (outer diameter) The designed dimensions of these hollow cylindrical samples were 80 mm (outer diameter) × (40 mm (height) × 2 mm (thickness), and the layer width was designed as 5 mm. The images were captured from side and top views using the 3D-SLSS.

The color differences indicate the distance of the surfaces of objects from the camera light source. For example, yellow represents the closest distance from the camera to the sample surface in a side view, and blue represents the farthest distance of the surface of the sample from the camera light source. If the printed sample was perfectly cylindrical, the middle portion of the printed samples in the side view should be the closest to the 3D-SLSS camera, showing yellow on the center line and other colors symmetrical to the center line. If the sample was printed with uniform width and well-leveled, the top view image of the samples should show a uniform color (40 mm [height] × 2 mm [thickness], with the layer width designed as 5 mm).

However, Figure 7.3 shows that none of the tested samples had a color distribution symmetrical to the center line, suggesting that they are not perfectly cylindrical. The top view images did not show uniform color either, implying the top layer filaments were not well-leveled, and the width

of the samples were not perfectly uniform. Among the three samples studied, the 3D-SLSS images of Sample 1 appeared the best, showing a relatively regular shape and uniform color distribution. The 3D-SLSS images of Samples 2 and 3 showed clear distortion in shape and large differences in color, and non-uniform color distribution, signifying a poorer 3D printing quality than Sample 1.

To measure the geometry of the 3D printed samples, e.g., layer thickness, layer width, surface roughness, and degree of distortion, the 3D images of the printed samples were sliced, and 16 different 2D plots were obtained (Figure 7.4).

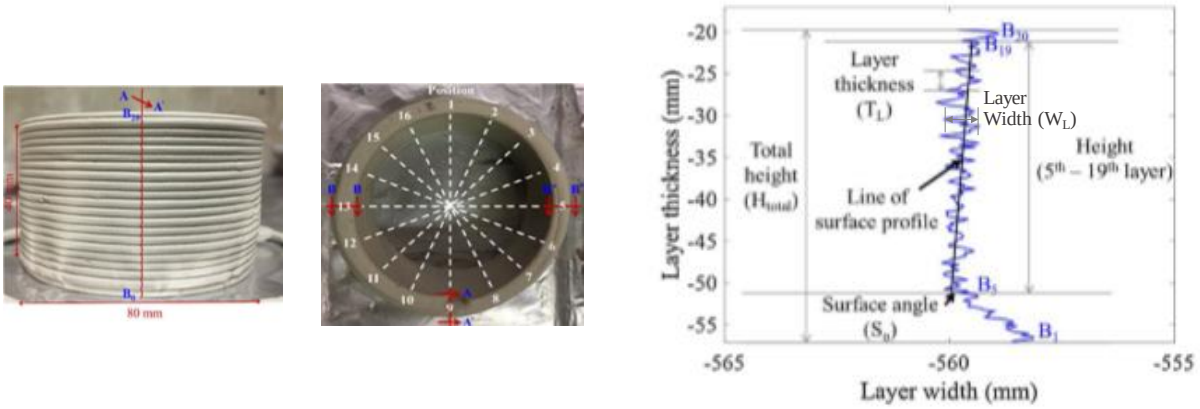

(a) Side view (b) Top view (c) Sample of 2D plot

Figure 7.4. Illustration of 2D plot development from 3D-SLSS images of a 3D printed sample

From these 2D plots, the geometrical parameters (total height, layer thickness, layer width, etc.) of the 3D printed samples were assessed.

Figure 7.5 shows the geometrical parameters of the 3D printed samples measured from the 3D-SLSS images. The measurements were compared with corresponding designed values. The figure demonstrates that none of the 3D printed samples had any geometrical parameter meeting the designed value, even for Sample 1, which had a very good visual appearance.

In the present study, the designed object height was 40 mm, but the height measurements of all 3D printed samples were below 40 mm (Figure 7.5a).

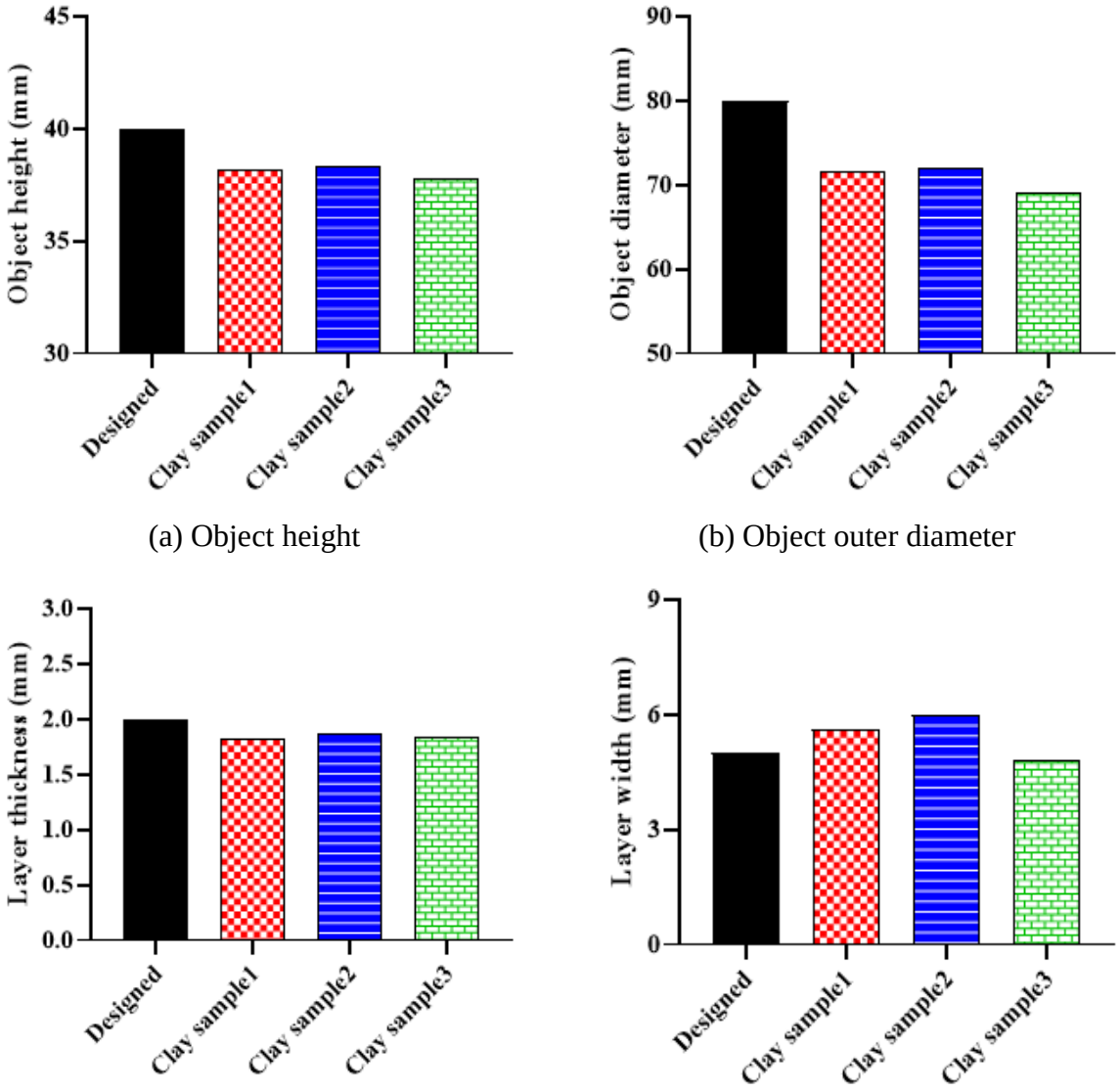

(a) Object height (b) Object outer diameter

(c) Layer thickness (d) Layer width

After Wi et al. 2020, *Additive Manufacturing*

Figure 7.5. 3D-SLSS measurements of geometric parameters of 3D printed samples

This may be because the printed clay filaments did not develop sufficient stiffness in time to resist the weight of the subsequently deposited filaments, thus causing slump and/or distortion.

Figure 7.5b shows that the outer diameters of all 3D printed samples were less than the designed value of 80 mm. This could partially result from a printer-related error by which the printing mortar did not deposit to the positions as designed. Distortion of the objects at an early stage of the printing process, e.g., the bottom layers in Samples 2 and 3 (Figure 7.3, side view), could also cause the average diameters of the printed objects to be different from the designed value.

Figure 7.5c illustrates that the average layer thickness measurements of the 3D printed samples were all slightly smaller than the designed value of 2 mm. However, Figure 7.5d shows that the layer widths of two out of the three 3D printed samples were larger than the designed value, 5 mm. This was because each layer of filament deformed under the weight of the subsequently deposited layers, which compressed the filaments, reducing the layer thickness and widening the layer width.

8. SUMMARY, CONCLUSION, AND FUTURE STUDY

8.1 Summary

The following activities were conducted in this research project:

1. A literature review was conducted to learn about 3D printing methods, equipment, materials, processes, and characterizations of printed products. Definitions of key properties of 3D printing concrete, e.g., printability, extrudability, buildability, flowability, pumpability, and open time, were clarified.

2. Before the arrival of a commercial 3D concrete printer, a plastic syringe was used to simulate the printing process and different materials were explored to identify the effects of materials on concrete printing. It was observed that silica fume and VMAs could enhance the buildability, and superplasticizer could increase flowability. The tests indicated that it was important to develop a mix proportion using different materials.

3. For 3D concrete printing, a commercial 3D clay printer was purchased. The platform moves along an x- and y-axis, and the printer head with the extruder moves along a z-axis. Moreover, the printer has its own control box, which users can employ to directly control extrusion and printing speeds.

4. Printing parameters, such as printing speed, extrusion speed, stand-off distance, and nozzle size and shape, could affect the printing qualities of printed objects. In this study, printing speed and extrusion speed were chosen to investigate the effects of printing parameters on the printing qualities with clay. It was observed that both affected the geometry of printed objects, and it indicated that the combination of printing and extrusion speeds is important for 3D printing.

5. Through trial printing with the plastic syringe, it was confirmed that the dosages of VMA and superplasticizer are important to printing cylindrical objects. As the dosage of VMA increased, extrudability decreased. Conversely, as the dosage of superplasticizer increased, flowability was enhanced. However, if the flowability increased, buildability decreased. Therefore, it was important to balance the flowability and buildability by using different materials and changing mix proportions.

6. Grout containing CSA cement, powder-form superplasticizer, filler, and various additives was incorporated into the mix design, since it could increase flowability and buildability due to the superplasticizer and CSA cement. By printing a cylindrical object, it was confirmed that a w/b ratio of 0.32 and 20% grout by weight (0.32-G20) was the best mix design.

7. The compressive strength of the printed samples was lower than that of the mold-cast sample, and the perpendicular strength was greater than the parallel, showing anisotropic behavior. This could be due to the fact that the interlayers created during the printing process acted as weak zones and decreased the compressive strength. However, the flexural strength of the printed samples was higher than that of the mold-cast sample. It's possible that the mixtures were compacted when they were extruded from the extruder and their microstructure was densified by the pressure.

8. Based on the ranking system developed in the present study, the research team's printed samples could be ranked as 2, meaning a printed object has rather uniform layers and a bit of a rough surface. In addition, a qualitative method with a 3D-SLSS to assess the printing qualities was developed.

8.2 Conclusions

The following are major conclusions drawn from the present study:

1. Due to the layer-by-layer additive manufacturing manner, different properties were required for 3D printing concrete rather than those from conventionally mold-cast concrete. The key properties for printable concrete mixtures include flowability, printability, extrudability, buildability, and open time. The 3D printable concrete mixtures should have suitable flowability in order to be easily transported from a mixer to a printer. They should have proper extrudability in order to be extruded out smoothly and consistently. Finally, the mixtures should develop sufficient stiffness to hold the object's shape or resist the weight of the subsequently deposited filaments without distortion or collapse.

2. The requirements for flowability, printability, extrudability, buildability, and open time of 3D printable concrete mixtures vary with the features of the printer used and the objects to be printed, and they also differ from printing parameters (deposition distance, extrusion speed, and printing speeds) and printing procedures (loading of printing material and design of printing paths) used. Therefore, the 3D printing concrete mixtures should be designed and adjusted to fit these features, parameters, and procedures.

3. Results from the literature review indicated that at present, cement pastes and mortars are the most commonly used 3D concrete printing materials. Various types of cement (portland cement and rapid-setting cement), supplementary cementitious materials (fly ash, silica fume, limestone powder, etc.), superplasticizers, and accelerators are frequently used in 3D printing concrete. The w/b ratio and s/b ratio of 3D printable concrete are often in the ranges of 0.30–0.40 and 1.0–1.5, respectively.

4. The present study suggests that the use of a highly flowable, rapid-setting grout that is commercially available to replace cement can simplify the 3D printing mortar mix design and achieve proper extrudability and buildability very effectively. Based on the test results, Mix 0.32-G20, made with a binder containing portland cement, silica fume (2.5% by weight of binder), and 20% grout and a w/b ratio of 0.32, showed satisfactory flowability, extrudability, and printability when a 3D potter printer was used for 3D concrete printing. The flow table test results showed that Mix 0.32-G20 had a final flow spread of 220 mm immediately after completion of mixing; 180 mm after 40 min rest, when printing/extrusion started; and 176 mm after 60 min. rest, when printing/extrusion was completed. This mixture was easily placed into the printer, extruded out smoothly and consistently, and able to hold the shape of the designed objects during and after printing.

5. Several defects were identified during the 3D concrete printing, and they were (a) air bubble pop outs, (b) discontinuity, (c) slumping, and (d) cracking. The first three were largely related to the flow behavior of the 3D printing concrete mixtures, while the last one was mainly due to plastic shrinkage. Prompt and proper curing is essential for 3D printing concrete in order to reduce slump and plastic shrinkage cracking.

6. The compressive and flexural strength of the 3D printing concrete were measured, and the results were compared with those of mold-cast samples. In order to take into account the direction of filaments, printed samples were loaded in two different directions (perpendicular and parallel to the printed filament). It was found that the mold-cast sample had a higher compressive strength than the printed samples regardless of loading directions. This might be attributed to the existence of interlayers between printed filaments. However, under flexural loading, the printed samples had a higher flexural strength than the mold-cast sample regardless of loading directions. Similar observations also had been made by other researchers. One explanation might be that the mixtures were densified during the 3D printing/extrusion process, leading to higher flexural strength when the 3D printed samples were loaded in the direction perpendicular to the filaments. However, little explanation could be made on why the 3D printed samples had higher flexural strength than the cast samples when they were loaded parallel to the filaments. Further study on this subject is necessary.

7. The 3D printed samples displayed different compressive and flexural strength values when loaded in different directions, which provided clear evidence of the anisotropic behavior of the bulk material. The compressive strength of the 3D printed samples loaded in the direction parallel to the filaments was much lower than that of the corresponding samples loaded in the direction perpendicular to the filaments, which was probably due to potential buckling of the filaments under compression. However, the difference in flexural strength of the 3D printed samples loaded in the two different directions was much smaller.

8. In order to evaluate the quality of the 3D printed concrete objects, a qualitative ranking system based on visual inspection was developed in the present study. Based on this ranking system, the samples printed with the best mortar mixtures used in the present study could be ranked as 2, since they showed uniform layers and a bit of a rough surface. Quantitative evaluation for the printing qualities was also conducted with a 3D-SLSS. The results showed that all the printed samples exhibited certain differences between their measured and designed values, even for those that appeared well-printed. Compared with the designed object, the printed samples generally had reduced total height, diameter, and layer thickness but increased layer width, mainly due to slump. In addition to printing materials (concrete mixtures), various printing parameters, including printing speed, extrusion speed, nozzle size and shape, stand-off distance, etc., could affect the printing qualities of the 3D printed objects. These affecting parameters should be further studied to improve the 3D printing quality.

8.3 Further Study

The goal of the further study is to transfer the startup research as presented in this report to scaleup research.

Through the present exploration study, the research team has gained sufficient experience to develop mortar mixtures that will be able to print "structural components" with a larger printer. The research team has investigated some commercially available 3D printer candidates, such as gantry, crane, and robot arm systems, and a Delta 3D printer, and learned their features, advantages, and limitations. Selection of an intermediate-sized robot arm with a mixing-pumping system is now under a special consideration due to its flexibility and functions.

Using a larger 3D printer, the research team will study properties of various mortar or concrete mixtures made with various materials, including various types and contents of fibers. Objects, such as columns and beams with a dimension around 3–4 ft will be printed and used for structural performance. The feasibility for printing small-scale structure components, such as small frames, slabs, and joints/connections, will also be explored, and the properties of these printed components will also be evaluated.

It is expected that this continued study will lead to the development of the scalability that links the behaviors of the small-scale 3D printing objects as conducted in the present project with the intermediate (pilot) scale and to provide a solid foundation for transferring the research results to full scale production.

REFERENCES

Ahmaruzzaman, M. 2010. A Review on the Utilization of Fly Ash. *Progress in Energy and Combustion Science*, Vol. 36, No. 3, pp. 327–363.

ArchDaily. 2017. Office of the Future / Killa Design. *ArchDaily*. https://www.archdaily.com/875642/office-of-the-future-killa-design?ad_medium=gallery.

Benaicha, M., X. Roguiez, O. Jalbaud, Y. Burtschell, and A. H. Alaoui. 2015. Influence of Silica Fume and Viscosity Modifying Agent on the Mechanical and Rheological Behavior of Self Compacting Concrete. *Construction and Building Materials*, Vol. 84, pp. 103–110.

Bentz, D. P., S. Z. Jones, I. R. Bentz, and M. A. Peltz. 2019. Towards the Formulation of Robust and Sustainable Cementitious Binders for 3D Additive Construction by Extrusion. *3D Concrete Printing Technology*, Vol. 2019, pp. 307–331.

Berodier, E. and K. Scrivener. 2014. Understanding the Filler Effect on the Nucleation and Growth of C-S-H. *Journal of the American Ceramic Society*, Vol. 97, No. 12, pp. 3764–3773.

Block, I. 2018. Robots Complete Span of 3D-Printed Bridge for Amsterdam Canal. *Dezeen*. https://www.dezeen.com/2018/04/17/mx3d-3d-printed-bridge-joris-laarman-arup-amsterdam-netherlands/.

Chandra, S. and J. Björnström. 2002. Influence of Cement and Superplasticizers Type and Dosage on the Fluidity of Cement Mortars—Part I. *Cement and Concrete Research*, Vol. 32, No. 10, pp. 1605–1611.

Harkins, G. 2019 The Marines Just 3D-Printed an Entire Bridge in California. *DOD Buzz Military News*. https://www.military.com/dodbuzz/2019/01/31/marines-just-3d-printed-entire-bridge-california.html.

Hong, J., K. Wang, Z. Xiong, M. Gong, C. Deng, G. Peng, and H. Zhu. 2019. Investigation into the Freeze–Thaw Durability of Semi-Flexible Pavement Mixtures. *Road Materials and Pavement Design*, pp. 1–17.

Institute for Advanced Architecture of Catalonia. 2017. World's First 3D Printed Pedestrian Bridge Built in Catalonia. *Designboom*. https://www.designboom.com/technology/worlds-first-3d-printed-pedestrian-bridge-catalonia-24-01-2017/.

Kazemian, A., X. Yuan, E. Cochran, and B. Khoshnevis. 2017. Cementitious Materials for Construction-Scale 3D Printing: Laboratory Testing of Fresh Printing Mixture. *Construction and Building Materials*, Vol. 145, pp. 639–647.

Khalil, N., G. Aouad, K. El Cheikh, and S. Rémond. 2017. Use of Calcium Sulfoaluminate Cements for Setting Control of 3D-Printing Mortars. *Construction and Building Materials*, Vol. 157, pp. 382–391.

Khoshnevis, B. and R. Dutton. 1998. Innovative Rapid Prototyping Process Makes Large Sized, Smooth Surfaced Complex Shapes in a Wide Variety of Materials. *Materials Technology*, Vol. 13, No. 2, pp. 53–56.

Khoshnevis, B. 2004. Automated Construction by Contour Crafting—Related Robotics and Information Technologies. *Automation in Construction*. Vol. 13, No. 1, pp. 5–19.

Kovler, K. 1998. Setting and Hardening of Gypsum-Portland Cement-Silica Fume Blends, Part 1: Temperature and Setting Expansion. *Cement and Concrete Research*, Vol. 28, No. 3, pp. 423–437.

Le, T. T., S. A. Austin, S. Lim, R. A. Buswell, A. G. Gibb, and T. Thorpe. 2012a. Mix Design and Fresh Properties for High-Performance Printing Concrete. *Materials and Structures*, Vol. 45, No. 8, pp. 1221–1232.

Le, T. T., S. A. Austin, S. Lim, R. A. Buswell, R. Law, A. G. Gibb, and T. Thorpe. 2012b. Hardened Properties of High-Performance Printing Concrete. *Cement and Concrete Research*, Vol. 42, No. 3, pp. 558–566.

Lee, H., W.-W. Kim, and J.-H. Moon. 2018. Study on Rheological Properties of Mortar for the Application of 3D Printing Method. *Journal of the Korean Recycled Construction Resources Institute*, Vol. 6, No. 1, pp. 16–24.

Leemann, A. and F. Winnefeld. 2007. The Effect of Viscosity Modifying Agents on Mortar and Concrete. *Cement and Concrete Composites*, Vol. 29, No. 5, pp. 341–349.

Lim, S., R. A. Buswell, T. T. Le, S. A. Austin, A. G. F. Gibb, and T. Thorpe. 2012. Developments in Construction-Scale Additive Manufacturing Processes. *Automation in Construction*, Vol. 21, pp. 262–268.

Ma, T., R. Yang, Z. Zheng, and Y. Song. 2017. Rheology of Fumed Silica/Polydimethylsiloxane Suspensions. *Journal of Rheology*, Vol. 61, No. 2, pp. 205–215.

Ma, G., Z. Li, and L. Wang. 2018. Printable Properties of Cementitious Material Containing Copper Tailings for Extrusion Based 3D Printing. *Construction and Building Materials*, Vol. 162, pp. 613–627.

Malaeb, Z., H. Hachem, A. Tourbah, T. Maalouf, N. El Zarwi, and F. Hamzeh. 2015. 3D Concrete Printing: Machine and Mix Design. *International Journal of Civil Engineering*, Vol. 6, No. 6, pp. 14–22.

Marchment, T., J. Sanjayan, and M. Xia. 2019. Method of Enhancing Interlayer Bond Strength in Construction Scale of 3D printing with Mortar by Effective Bond Area Amplification. *Materials and Design*, Vol. 169, 107684.

Mardani-Aghabaglou, A., M. Tuyan, G. Yılmaz, Ö. Arıöz, and K. Ramyar. 2013. Effect of Different Types of Superplasticizer on Fresh, Rheological, and Strength Properties of Self-Consolidating Concrete. *Construction and Building Materials*, Vol. 47, pp. 1020–1025.

Massachusetts Institute of Technology. 2017. System Can 3-D Print an Entire Building: Tech Could Enable Faster, Cheaper, More Adaptable Building Construction. *ScienceDaily*. https://www.sciencedaily.com/releases/2017/04/170426183028.htm.

Mehdipour, I. and K. H. Khayat. 2017. Effect of Particle-Size Distribution and Specific Surface Area of Different Binder Systems on Packing Density and Flow Characteristics of Cement Paste. *Cement and Concrete Composites*, Vol. 78, pp. 120–131.

Oey, T., A. Kumar, J. W. Bullard, N. Neithalath, and G. Sant. 2013. The Filler Effect: The Influence of Filler Content and Surface Area on Cementitious Reaction Rates. *Journal of the American Ceramic Society*, Vol. 96, No. 6, pp. 1978–1990.

Ogura, H., V. N. Nerella, and V. Mechtcherine. 2018. Developing and Testing of Strain-Hardening Cement-Based Composites (SHCC) in the Context of 3D-Printing. *Materials*, Vol. 11, No. 8, pp. 1–18.

Ravenscroft, T. 2019. World's Longest 3D-Printed Concrete Bridge Opens in Shanghai. *Dezeen*. https://www.dezeen.com/2019/02/05/worlds-longest-3d-printed-concrete-bridge-shanghai/.

Rogers, J. 2018. Marines 3D-Print Concrete Barracks in Just 40 Hours. *Fox News Proud American*. https://www.foxnews.com/tech/marines-3d-print-concrete-barracks-in-just-40-hours.

Sevenson, B. 2015. Shanghai-Based WinSun 3D Prints 6-Story Apartment Building and an Incredible Home. *3DPrint.COM*. http://3dprint.com/38144/3d-printed-apartment-building/.

Soltan, D. G. and V. C. Li. 2018. A Self-Reinforced Cementitious Composite for Building-Scale 3D Printing. *Cement and Concrete Composites*, Vol. 90, pp. 1–13.

Vaitkevičius, V., E. Šerelis, and V. Kerševičius. 2018. Effect of Ultra-Sonic Activation on Early Hydration Process in 3D Concrete Printing Technology. *Construction and Building Materials*, Vol. 169, pp. 354–363.

Wang, D., C. Shi, N. Farzadnia, Z. Shi, H. Jia, and Z. Ou. 2018. A Review on Use of Limestone Powder in Cement-Based Materials: Mechanism, Hydration and Microstructures. *Construction and Building Materials*, Vol. 181, pp. 659–672.

Wang, K. and J. Hong. 2019. *Hybrid Concrete for Advancing Pavement Performance*. Midwest Transportation Center, Institute for Transportation, Iowa State University, Ames, IA. https://intrans.iastate.edu/app/uploads/2019/03/hybrid_concrete_for_pvmt_performance_w_cvr.pdf.

Wi, K., V. Suresh, K. Wang, B. Li, and H. Qin. 2020. Quantifying Quality of 3D Printed Clay Objects Using a 3D Structured Light Scanning System. *Additive Manufacturing*, Vol. 32, 100987.

Wu, P., J. Wang, and X. Wang. 2016. A Critical Review of the Use of 3-D Printing in the Construction Industry. *Automation in Construction*, Vol. 68, pp. 21–31.

Zhang, Y., Y. Zhang, G. Liu, Y. Yang, M. Wu, and B. Pang. 2018. Fresh Properties of a Novel 3D Printing Concrete Ink. *Construction and Building Materials*, Vol. 174, pp. 263–271.

Zhang, Y., Y. Zhang, W. She, L. Yang, G. Liu, and Y. Yang. 2019. Rheological and Harden Properties of the High-Thixotropy 3D Printing Concrete. *Construction and Building Materials*, Vol. 201, pp. 278–285.

Zhi, Z., B. Ma, H. Tan, Y. Guo, Z. Jin, H. Yu, and S. Jian. 2018. Effect of Competitive Adsorption between Polycarboxylate Superplasticizer and Hydroxypropylmethyl Cellulose on Rheology of Gypsum Paste. *Journal of Materials in Civil Engineering*, Vol. 30, No. 7, 04018141.

THE INSTITUTE FOR TRANSPORTATION IS THE FOCAL POINT FOR TRANSPORTATION AT IOWA STATE UNIVERSITY.

InTrans centers and programs perform transportation research and provide technology transfer services for government agencies and private companies;

InTrans contributes to ISU and the College of Engineering's educational programs for transportation students and provides K–12 outreach; and

InTrans conducts local, regional, and national transportation services and continuing education programs.

IOWA STATE UNIVERSITY

Visit **InTrans.iastate.edu** for color pdfs of this and other research reports.